29. PHYSICAL PROPERTIES OF SEDIMENT AND ROCKS FROM THE D'ENTRECASTEAUX COLLISION ZONE AND NORTH AOBA BASIN, VANUATU ISLAND ARC[1]

John N. Leonard[2] and Maria V.S. Ask[3]

ABSTRACT

Physical properties measurements from seven Ocean Drilling Program (ODP) Leg 134 sites in the area where the twin submarine ridges of the d'Entrecasteaux Zone (DEZ) collide with the New Hebrides Island Arc document the subduction processes in the central New Hebrides Trench. The North d'Entrecasteaux Ridge (NDR) and South d'Entrecasteaux Chain (SDC) appear to clog the trench, uplifting Espiritu Santo Island at a rapid rate and helping to form the North Aoba Basin (NAB), a deep depression of the Pacific Plate that traps eroded sediment and ash from the surrounding island volcanoes. Porosity and water content measurements indicate that significantly less fluid exists in the Vanuatu accretionary complex than at other prisms (Barbados and Nankai). This is due, in part, to lithologic differences of sediments being incorporated into the complex from the DEZ, which are more coarse-grained, less porous, and more permeable than the hemipelagic clay-dominated Barbados forearc. Velocity anisotropy observed in the DEZ and NAB at Sites 827–833 suggests that tectonically induced lateral compression is taking place, resulting in pore volume reduction, sediment strengthening, and dewatering of the collision complex through fault-controlled fracture permeability. More fluids and higher porosity material bracketing indurated rocks in the NAB are evidence of rapid burial and alteration of sediment during intense bursts of volcanism associated with tectonic subsidence of the basin, and/or surrounding island belts due to arc-wide lateral compression from collision.

INTRODUCTION

ODP Leg 134 investigated the different styles of deformation occurring in the region of collision between the twin submarine ridges of the d'Entrecasteaux Zone (DEZ) and Central New Hebrides Island Arc. In the Vanuatu area, the Australia Plate subducts eastward beneath the Pacific Plate at a rate of 13 cm/yr, forming the New Hebrides Trench (Fig. 1; Taylor et al., this volume). The DEZ, which also is moving northward at 3–4 cm/yr (Greene et al., this volume), comprises two different features: the continuous, aseismic North d'Entrecasteaux Ridge (NDR), and the South d'Entrecasteaux Chain (SDC), a discontinuous line of seamounts. Active accretion with the twin-ridge system of the DEZ complicates subduction in the Central New Hebrides Trench. The NDR and SDC each impinge upon the Vanuatu island arc, clogging the trench and causing different styles of deformation that drastically alter the arc's physiography and structure. Mountainous islands (Espiritu Santo, Malakula) have risen adjacent to the trench. In the backarc area an extensional province disappears abruptly, and the large, intra-arc Aoba Basins are substantially deeper than any other basin in this island arc system (ODP Leg 134 Drilling Party, 1991). The mechanics and hydrologic processes of how the collision affects accretion, the age of collision, and a proposed reversal of subduction polarity that may have helped form the unusual three chains of volcanic islands in the arc, stimulated interest in studying this unique area and comparing the results with those from other convergent margins.

Shipboard determinations of physical properties are the basis for geotechnical stratigraphy studies and provide the essential link between geophysical seismic survey data, downhole electrical logging results, and the visual geologic record obtained by coring. The combination of these three data sets provides the clearest integrated view of the sub-seafloor conditions surrounding the bore hole. The detailed study of the physical properties associated with collision complements

the three principal objectives of Leg 134. Locations chosen for drilling focused on three important and poorly understood aspects of this arc system: (1) the different styles of deformation below the seafloor where the twin ridges of the DEZ collide with the arc; (2) the evolution and shifting of the magmatic arc between the three island chains since the possible reversal of subduction polarity in the Miocene; and (3) dewatering of the forearc and subducted lithosphere from evidence provided by geotechnical and geochemical investigation of the sediment, rocks, and pore water. Two of the three primary objectives of Leg 134 are central to the research described in this paper. These two objectives were to quantify the general physical and geotechnical properties of the sediment and rocks, and how those properties relate to the structural geology of accreted sequences and the different styles of forearc deformation caused by collision of the arc with the NDR and the SDC; and to document the water content, dewatering processes, and fluid migration pathways in the sediment and rocks and compare differences in these processes between the d'Entrecasteaux Zone (DEZ) accretion/collision complex and the undeformed, rapidly deposited sediments in the North Aoba Basin (NAB).

Our working hypothesis at the outset of Leg 134 was that porous, fluid-rich, well lubricated clays, which are probably high in smectite and very low in calcium carbonate content, might be the locus of slip that forms the décollement at all convergent margins that have an accretionary prism. Comparisons are made between Leg 134 accretionary drilling results and earlier drilling results, particularly those from the Barbados and Nankai prisms. Measurements of physical properties and geotechnical analyses are the principal means of defining these processes, which also serve to help explain structural characteristics found in cores and observed on seismic cross sections.

Sites 827–831 were drilled in the active collision zone of the central New Hebrides Island Arc to define the internal deformation of a forearc slope colliding with aseismic ridges. Broad-scale deformation patterns differ significantly at the two sites where the NDR and the Bougainville Guyot, the easternmost seamount in the SDC, impact with the arc. To document the mechanics and hydrologic processes associated with accretion and collision, Sites 827, 828, and 829 were located on the NDR, while Sites 830 and 831 were situated around Bougainville Guyot (Fig. 1).

Another set of drill sites, Sites 832 and 833, were chosen to document the evolution of the NAB (Fig. 1; i.e., to determine the exact age
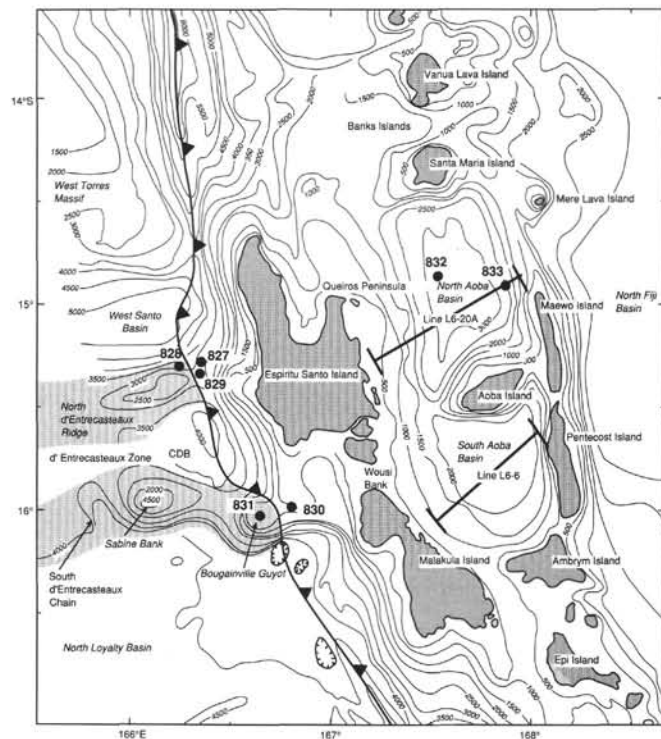
Figure 1. Map showing the locations of Leg 134 Sites 827–833, where the twin submarine ridges that form the d'Entrecasteaux Zone (DEZ) collide with the central New Hebrides Island Arc (Vanuatu).

of the collision and to document the hypothesized Miocene-age reversal of subduction polarity from the inactive Vitiaz Trench to the current New Hebrides Trench). The summit basins of the New Hebrides Island Arc form a nearly continuous north-south "median sedimentary basin" of Luyendyk et al. (1974), which is broken only by the active volcanoes of the Central Chain. The Central Chain volcano forming Aoba Island divides the North and South Aoba Basins, which has greater bathymetric expression than any other basins on the New Hebrides arc summit (Katz, 1988). The oblique collision of the DEZ caused large transverse, transcurrent fractures throughout central Vanuatu (Greene et al., 1988). These wrench faults are major elements in the area's Quaternary structural pattern because they have allowed migration of undifferentiated mantle-derived magma to form the Central Chain islands of Aoba and Ambrym (Greene et al., 1988; Briqueu, this volume). Continued collision with the DEZ is thought to be deepening the Aoba Basins and/or elevating the surrounding island belts, causing rapid deposition of very underconsolidated sediment and ash from active volcanism and erosion of the surrounding island chains (Collot, Greene, Stokking, et al., 1992).

METHODS

Physical properties measurements are routinely performed aboard *JOIDES Resolution* on all cores immediately after recovery from the seafloor, according to the general procedures outlined by Boyce (1976), the ODP Shipboard Measurements Panel (9/30/90), and American Society of Testing and Materials (ASTM) 1989. Since Leg 134 was the third ODP cruise to attempt drilling through a décollement, in general our physical properties procedures replicated as closely as possible those of earlier cruises that penetrated décollements, Leg 110 (Barbados Ridge; Mascle, Moore, et al., 1988) and Leg 131 (Nankai Trough; Taira, Hill, Firth, et al., 1991). The parameters measured during the Leg 134 cruise included index properties (wet- and dry-bulk density, grain density, water content, and porosity,

sonic (compressional or shear wave) velocity, vane shear strength, and thermal conductivity. Calcium carbonate content (CaCO$_3$%) was measured in the shipboard geochemistry lab using the dried index properties samples. The sampling interval for discrete index property measurements was as frequent as physically possible, with 4–5 samples taken per full (9.5 m) recovery core and at least one sample per core when core recovery was low (0.1–9 m). Samples were taken in sections of least disturbance and in different lithologies representative of the entire core. Precise weight and volume measurements were made with an electronic balance and pycnometer, and entered in the computer. After calculation, obviously erroneous measurements were deleted from each data set. By convention in geotechnical engineering, the term "bulk density" usually refers to wet-bulk density and "porosity" to wet porosity, but "water content" refers to dry water content, or the weight of water relative to the weight of solids expressed as a percentage. Expressed this way, it is not unusual for water content values in marine sediment to be greater than 100%. Leg 134 wet water content values range from 1%–20% lower than dry values. Dry-density, porosity, and wet water content were tabulated but not used in our discussion. The complete physical properties methods and shipboard procedures are outlined in full detail in the "Physical Properties" section of the "Explanatory Notes" chapter of the Leg 134 *Initial Reports* (Collot, Greene, Stokking, et al., 1992).

Measurements of sonic velocity and undrained vane shear strength were made immediately adjacent (in the same 10 cm core interval) to index property measurements. Wherever possible, measurements for both were made parallel to the core axis (vertical) and perpendicular to the core axis (horizontal). Decreased recovery and increased state of lithification of the cores with depth prevented acquisition of quality shear strength data below 100–200 mbsf and resulted in many Leg 134 cores being recovered by Rotary Core Barrel (RCB) rather than Advanced Piston Corer (APC) method. Gamma-Ray Attenuation Porosity Evaluator (GRAPE) and thermal conductivity measurements were made on sections with good recovery. However, a full core liner is needed for accurate GRAPE data, and only soft, competent sediment and rocks will accommodate the thermal conductivity probe. Such APC-recovered intervals represent a limited number of the cores, so the GRAPE and thermal conductivity data are not discussed in this paper in detail.

Compressional and shear wave traveltimes and distances were measured in a velocimeter. Lithified, homogeneous sediment and hard rocks gave a more distinct signal than lithified heterogeneous or soft sediment. Soupy or incompetent sediment could not be properly measured, therefore, values for both vertical and horizontal velocity were not always obtained. For measurements in which the compressional velocity (V_p) signal was noisy, the shear velocity (V_s) was measured instead; these measurements are noted in the data. Calculations of vertical and horizontal anisotropy (A) use the equation of Carlson and Christensen (1977), who compared their results from the South Atlantic with Hamilton's (1970) Pacific data for compressional velocities:

$$A = 2 (V_h - V_v) (V_h + V_v)^{-1}$$

A values are negative when compressional velocity vertically is greater than horizontal ($V_v > V_h$). Shear waves are also plotted in the anisotropy figures; compressional waves are indicated by solid circles and shear waves are indicated by empty circles. In this paper, we call the sample isotropic when $A = 0$ and anisotropic when $|A| \leq 0.5\%$. The sample is called semi-isotropic when $0 < |A| < 0.5\%$.

Additional measurements of wet-bulk density, wet porosity, dry water content, grain density, and vane shear strength were performed on twenty-five 10-cm whole-round core samples collected for consolidation and permeability tests in the Marine Geotechnical Laboratory at Texas A&M University. Atterberg Limits tests were also performed to determine the water content ranges within which the sediments behave as solid, plastic, or liquid materials. All shorebased geotechnical data provided excellent correlation with the measurements made

aboard ship and are tabulated in Leonard, 1991. Shorebased data points are plotted along with the shipboard physical properties in the figures in this paper where noted.

This chapter will present the physical properties results sequentially from the DEZ collision sites on the NDR (Sites 827–829), the SDC (Sites 830, 831), and the NAB (Sites 832, 833). Complete tables of all Leg 134 Sites 827–833 physical properties data are contained in Collot, Greene, Stokking, et al. (1992).

Validation of the Data

Core recovery and the amount of core disturbance varied considerably across the seven sites. These variations reflect differences in stress regime and lithology, as well as the drilling method. Laboratory physical properties measurements are not made in situ, and cores that are not recovered by APC are of decreased quality for physical properties and geotechnical samples. Because of this, a validation of the reliability of the data was made by comparing the accuracy of the laboratory measurements with the corresponding downhole measurements. Logging data was acquired for five sites, 829–833 (Shipboard Scientific Party, 1992c–g). Among the downhole tools, the Rho-B channel (RHOB) of the High-temperature Lithodensity Tool (HLDT or LDT) measures the bulk density in situ and can thus be compared with discrete bulk density determinations measured in the laboratory.

Although the RHOB is fairly sensitive to borehole effects that can skew logging data, generally, RHOB-density log results correlate very well with the discrete shipboard laboratory values. The only exceptions are at the SDC sites: Site 830 (Guyot Collision), and the poorly recovered neritic carbonates of Site 831 on the Bougainville Guyot. Both RHOB and laboratory measurements follow the same trend for these sites, but the discrete bulk density values measured noticeably higher. RHOB-density log results depend on the borehole size: RHOB-density values tend to increase as the hole diameter decreases. At Sites 830 and 831, RHOB-logged densities are consistently at least 0.4 Mg/m³ lower than the bulk densities that were measured in the shipboard laboratory. In both cases, this difference was probably caused by a larger downhole diameter, which caused the RHOB measurements to decrease. Downhole measurement results will be referred to in the following discussion when appropriate for comparison.

RESULTS

North d'Entrecasteaux Ridge (NDR) Collision, Sites 827–829

Sites 827, 828, and 829 are the first three of a series of five Leg 134 sites (Sites 827–831; Fig. 1) drilled within the collision area of the DEZ. Sites 827 and 829 were attempts to penetrate through the accretionary complex to the décollement between the forearc slope of the New Hebrides Island arc and the sediment and rock units of the underlying NDR. Although it was drilled subsequent to Site 827, Site 828 will be discussed first because it was proposed as the reference site to document the extent of deformation that has occurred where the NDR collides with the central New Hebrides Island Arc. Sites 827 and 829 penetrated the accretionary wedge close to the reference site, across the deformation front from Site 828 at a distance of 2 km from the trench (Fig. 1).

Subduction of the NDR has formed a submarine lobe protruding westward from Espiritu Santo Island called Wousi Bank, which consists of uplifted forearc sediment and rocks and stacked thrust sheets accreted from the ridge (Greene et al., 1992). Due to hole instability problems at depth at each of the first three sites, the décollement was not reached, but drilling at Sites 827 and 829 recorded the first penetration by ODP of an accretionary complex in a subduction zone where a ridge collides with an island arc (Collot, Greene, Stokking, et al., 1992).

Site 828: NDR Reference

Site 828 is located about 2 km seaward of the New Hebrides Trench at 3086.7 mbsl on a terrace of the northern flank of the NDR. Geophysical surveys show a sedimentary cover beneath which basement rocks appear to lie within 300 m of the seafloor. Site 828 penetrated to a total depth of 129 m, with 109.3 m of sediment and brecciated, basement-like volcanic rock recovered before hole collapse forced the site to be abandoned. Four lithostratigraphic units were described, ranging from Pleistocene volcanic silt to Oligocene nannofossil chalk (Shipboard Scientific Party, 1992b). Cores from Site 828 give an excellent history of the sedimentation and tectonic movements of the ridge (Reid et al., this volume). Drilling confirms that the DEZ was an incipient subduction zone sometime in the Eocene. Basement volcanic rocks recovered appear to be middle Eocene in age. Most, if not all of the Miocene and uppermost Oligocene appears to be absent from the entire site, suggesting the ridge may have been emergent during that period (Leg 134 Shipboard Scientific Party, 1991). The Miocene section was also missing south of the DEZ in the North Loyalty Basin at Site 286 (Leg 30; Andrews, Packham, et al., 1975), the only previous DSDP drilling in this area.

With few exceptions, the physical properties at reference Site 828 trend uniformly downhole (Fig. 2). Porosity decreases only slightly downhole from an initial value of 59% as bulk density increases rapidly in the first few meters below seafloor (mbsf) from 1.8 Mg/m³; both values then remain steady through 58.7 m of volcanic silt unit (lithostratigraphic Unit I). From 58.7–61.9 mbsf, Unit IIA is a brown foraminiferal ooze with nannofossils and volcanic silt; in Unit IIB (61.9-69.3 mbsf), the foraminiferal ooze becomes white, wet, unconsolidated, and there is no volcanic component. Water content in the white ooze is 92.6% and porosity is 72.2%, by far the highest values at Site 828. The change in lithology can be seen in the sharp increase in $CaCO_3$ content. In the Oligocene nannofossil chalk from 69.3–90.8 mbsf (Unit III), bulk density and water content values are slightly variable. In general, water content in Unit III is higher than in the overlying Pleistocene volcanic silt (Unit I). In the volcanic breccia at 93.3 mbsf, water content is 22.3%, bulk density is a relatively low 2.15 Mg/m³, and velocity is less than 2000 m/s. Below 100 mbsf, the deepest rocks recovered from the NDR are middle Eocene(?) Mid-Ocean Ridge Basalt (MORB) and olivine dolerite clasts, which have measured densities of 2.81 Mg/m³ or more.

As with the index properties, few dramatic changes are seen in the sonic velocities measured at Site 828 (Fig. 2B). The velocities are semi-isotropic (e.g., less than 5% difference between horizontal and vertical velocity), and they decrease slightly with depth. Values vary between 1525–1652 m/s. Complete tables of values and figures for index properties, sonic velocities, vane shear strength, and thermal conductivity for all Leg 134 sites are contained in Collot, Greene, Stokking, et al. (1992).

Site 827: NDR Collision Site

Site 827 penetrated to a total depth of 400.4 mbsf and recovered 219.8 m of core comprising four lithostratigraphic units of tectonically deformed volcanic silt, sand, calcareous volcanic siltstone, sed-lithic conglomerate, and breccia from upper Pliocene to Pleistocene-Holocene in age (Reid et al., this volume). Due to hole collapse, Site 827 was abandoned before reaching the objective of the décollement (Shipboard Scientific Party, 1992a).

Physical properties at Site 827 show the effects of collision, but not nearly to the extent seen at Site 829. Figure 3 shows physical properties plotted along with structural features. Structural disruptions from tectonic effects were small or absent in the upper two lithostratigraphic units (0–141 mbsf). Index properties change little with depth, while velocity and carbonate content (Fig. 3) increase slowly in Units I and II. From 0–86 mbsf (Unit I), Holocene-Pleistocene volcanic silt
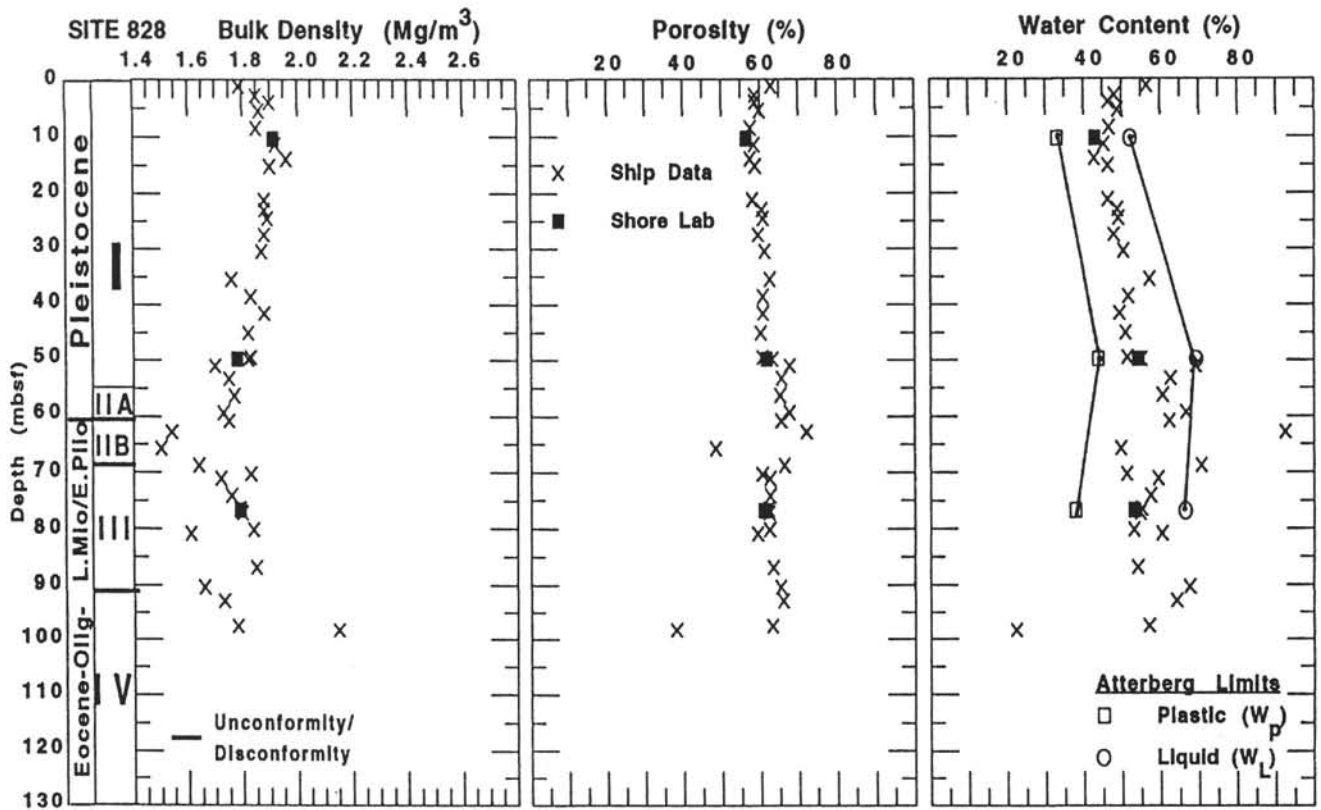
Figure 2. Physical properties plotted vs. depth for NDR reference Site 828, including age, lithostratigraphic units, and structural features. Noteworthy trends are discussed in the text.
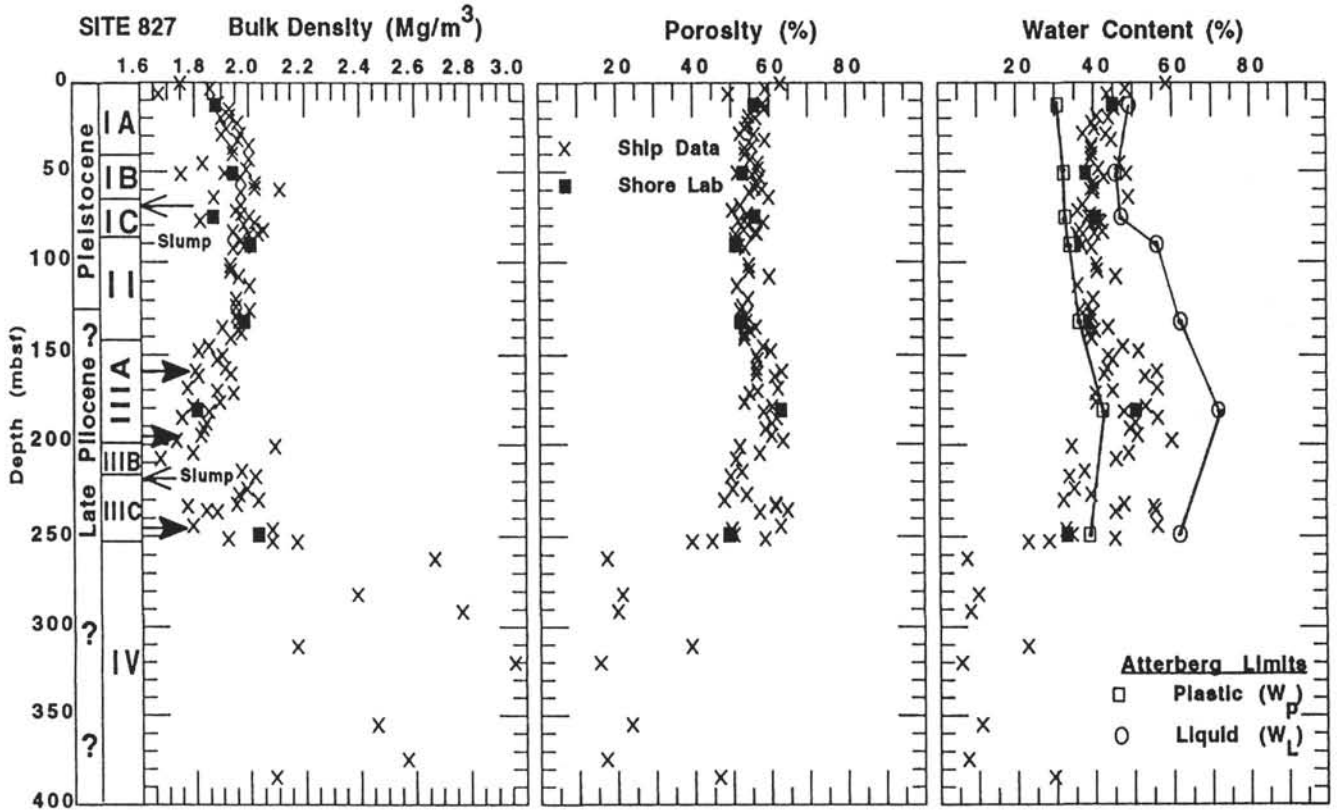

Figure 3. Physical properties plotted vs. depth for NDR collision Site 827, including age, lithologic units, and structural features (arrows). In sonic velocity and calcium carbonate content vs. depth figure, note correlation of thrust faults with zones that are low in CaCO$_3$%.
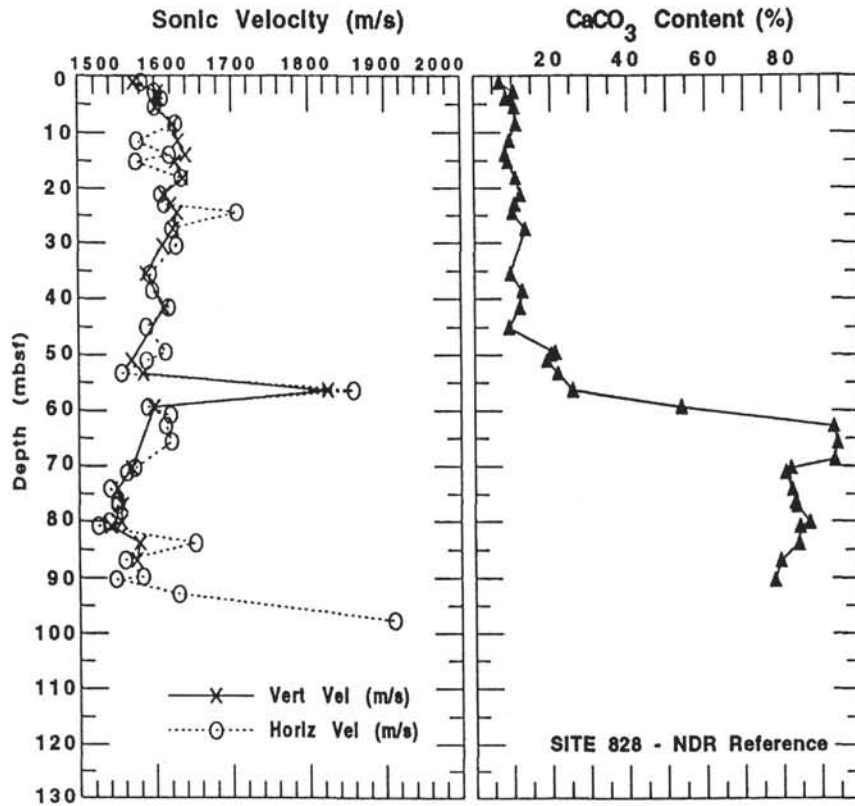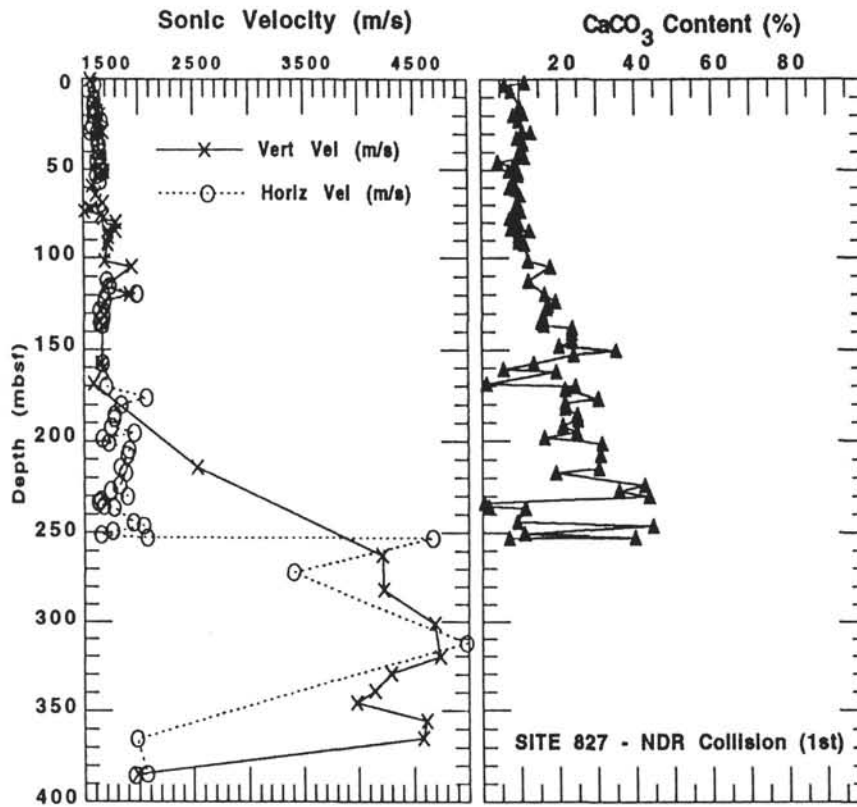
Figure 2 (continued).

Figure 3 (continued).

containing varying amounts of sandy turbidites shows no apparent tectonic deformation. Bulk density variations support evidence of a slump at 70 mbsf. At 107 mbsf, tectonic deformation is expressed as small-scale faults (Meschede and Pelletier, this volume), and this corresponds to a slight spike of about +5% in porosity and water content values at that depth, associated with the faults. Between 141–252 mbsf (Unit III), structural features such as scaly fabric and shear zones are common along with small faults, and the structural features correlate with variations in the physical properties. Bulk density decreases, and porosity and especially water content increase from 141–200 mbsf in calcareous volcanic siltstone with three intervals of sed-lithic conglomerate. Two shear zones, at 160 and 195 mbsf, are associated with progressively thicker sections of scaly cleavage. The shear zones are interpreted as thrust faults, but there are no evident or resolvable biostratigraphic reversals, and the thrust zones may be intraformational, caused by accretion (Reid et al., this volume; Meschede and Pelletier, this volume). The shear zones correlate particularly well with porosity and water content changes. Porosity and water content values increase and decrease abruptly in several locations (at 160 and 201 mbsf) (Fig. 3A) associated with thrust faults in the shear zones. A third major shear zone, with a biostratigraphic reversal, occurs at 243 mbsf, and once again is marked by an increase and then a sharp decrease in porosity and water content (Fig. 3A). Bulk density varies indirectly in this interval, decreasing and then sharply increasing in value (Table 5, "Site 827," Shipboard Scientific Party, 1992a).

Calcium carbonate content at Site 827 is approximately 10% at the seafloor and increases steadily downhole to about 50% at 250 mbsf (Fig. 3B), except for several sharp negative spikes of almost zero carbonate. Structural features, particularly thrust faults, seem to preferentially occur in the thin zones of low $CaCO_3$%, a pattern which is also observed at Site 829. Below 252 mbsf (Unit IV) in Hole 827B, drilling became difficult and core recovery very low, as sed-lithic conglomerate with pebble-sized clasts of volcanic breccia (andesite, dacite), siltstone, and sandstone was encountered to the total depth of the hole at 400.6 mbsf (Reid et al., this volume).

Site 829: NDR Collision

Site 829 was drilled as a second attempt to reach the décollement after the initial attempt at Site 827 had to be abandoned at a depth of 400 mbsf. The site was located 3 km south of Site 827, away from the terrace of ponded sediments, which may have contributed to the hole collapse that terminated Hole 827B (Shipboard Scientific Party, 1992a). Hole 829A, the deepest hole on the NDR, drilled into the accretionary complex to a total depth of 590 mbsf before collapsing due to hole instability. Although Site 829 had to be abandoned before the décollement was penetrated fully, we successfully cored the overlying thrust sheets and accretionary prism and may have entered the upper reaches of the décollement zone (Shipboard Scientific Party, 1992c; Fisher et al., this volume).

Hole 829A penetrated 517.2 m of marine sediment ranging in age from Pleistocene to Oligocene, overlying 73.1 m of volcanic breccia. The structural geology and lithostratigraphy are complex. Nine major thrusts and at least four smaller faults separate lithologic units containing progressive deformation and numerous biostratigraphic reversals downhole. Sixteen lithostratigraphic units are defined from Hole 829A on the basis of lithology, carbonate versus volcanic composition, and structural relationships (Reid et al.; Meschede and Pelletier, this volume).

The physical properties at Site 829 correlate extremely well with the lithostratigraphic units as defined by the tectonic deformation (Fig. 4). The 590 m sequence of the NDR accretionary complex is comprised of several sediment packages that are separated by thin clay layers. Of the eleven (9 major, 2 minor) thrust faults shown in Figure 4A, three are major shear zones (400, 462, and 518 mbsf), each
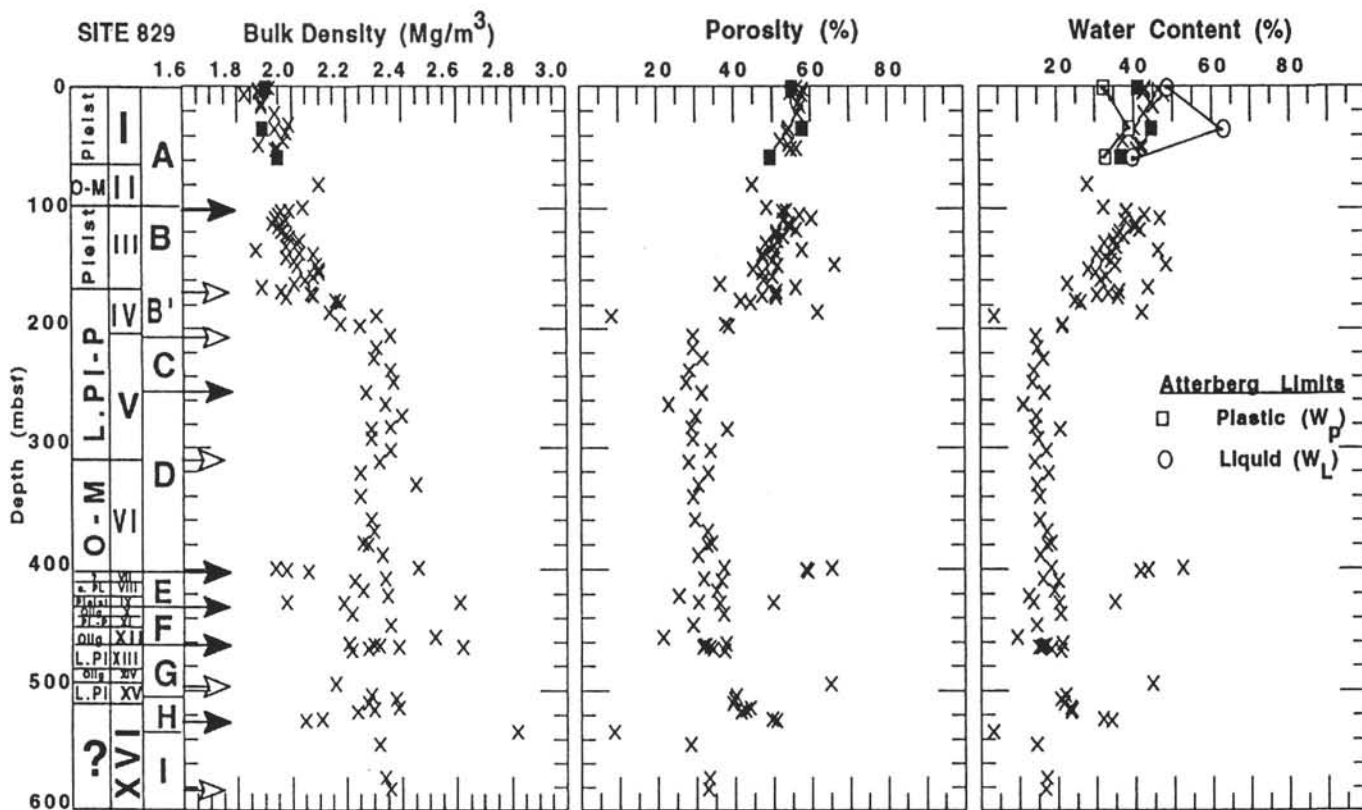

Figure 4. Physical properties vs. depth for NDR collision Site 829, including age, lithostratigraphic units, structural units, and major and minor shear zones (arrows). In sonic velocity and calcium carbonate content vs. depth figure, note correlation of thrust faults with zones that are low in $CaCO_3$%.

of which was initially when first penetrated thought to have been the décollement. Brown clay laminae only centimeters thick account for increased porosity and water content and decreased bulk density immediately above each thrust fault. These index properties then undergo reversals immediately below the faults, with values similar to values found at Site 827. The faults containing brown clay account for the wide scatter in index property values in the highly tectonized zone from 400–520 mbsf.

Relatively undeformed silt, siltstone, and chalk in the top interval from 0–170 mbsf (Units I–III) show a downhole decrease in water content, from 48% to 34%, and a corresponding decrease in porosity, from 58% to 50%. Upper Oligocene to lower Miocene foraminiferal chalk from 60.5–99.4 mbsf (Unit II) was poorly recovered, but one measurement suggests that the chalk is drier than the silt, with a water content of about 28% and a porosity of 45%. The first thrust fault at 99 mbsf is marked by increases in porosity and water content of nearly 20% at the fault plane. Below the fault, porosity, and water content values show more scatter, and decrease downhole to 170 mbsf.

The interval from 170–200 mbsf records a transition from relatively wet sediment above 170 mbsf to more lithified sediment and rocks below 200 mbsf that are much drier except at thrust faults. This is a highly deformed zone of sedimentary tectonic melange (Unit IV) composed of sheared chalk-siltstone breccia and characterized by wide-ranging values of water content (4%–40%) and porosity (8%–60%). Below 200 mbsf, sediment and rocks have very low porosity (20%–30%) and water content (10%–20%). These units (V–XVI), highly deformed and sheared chalk breccia, chalk and volcanic breccia, siltstone, sandstone, and silty chalk, show sudden increases in porosity and water content of 20% or more in thrust fault intervals, particularly in the three major shear zones from 400–600 mbsf. The very highly sheared interval from 400–500 mbsf also has wide swings in CaCO$_3$%. Fluid yields from samples squeezed for pore water below 200 mbsf corroborate these data (Shipboard Scientific Party, 1992c;

Martin, this volume); the whole-round core samples were virtually dry except for those collected immediately below thrust faults, which yielded small amounts of water.

Physical properties results also correlate with the interpreted origins of the sedimentary packages (Reid et al., this volume; Meschede and Pelletier, this volume) from the seafloor to the bottom of Hole 829A, in the following manner: (1) accreted ridge sediments with a drape of in-situ slope sediment from 0–99.4 mbsf; (2) accreted ridge material overlain by accreted trench fill deposits (99.4–405 mbsf); (3) slivers of ridge overlain by trench fill from 405 to 517 mbsf (the most tectonized zone in the hole), alternating with (4) pieces of ridge scraped off the volcanic basement at the brown clay layers; and (5) accreted ridge basement material (517–590 mbsf), lithologically similar to volcanic breccia from Site 828 (Coltorti, et al., this volume). Tectonic effects are particularly evident in compressional velocity anisotropy data. Figure 5 shows that anisotropy is greater with depth at Site 829 than at Sites 828 and 827. In the unaccreted sediments at the first two sites and in the upper 100 m of Site 829, less anisotropy can be attributed to the volcanic nature of the sediments and the rapid sedimentation rate. At Site 828, A values are very slightly negative, meaning $V_v > V_h$. At Site 827, slightly negative anisotropy reverses to slightly positive below 107 mbsf, as lateral tectonic deformation begins to appear. In the accreted sediment at Site 829, the larger range of anisotropy is almost certainly due to the great degree of tectonization, which causes the more chaotic pattern in the data below 170 mbsf.

South d'Entrecasteaux Chain (SDC) Collision, Sites 830–831

Site 830: SDC Collision

Site 830 is in 1020 m of water, 6.5 km east of the plate boundary where Bougainville Guyot, the easternmost member of the SDC,
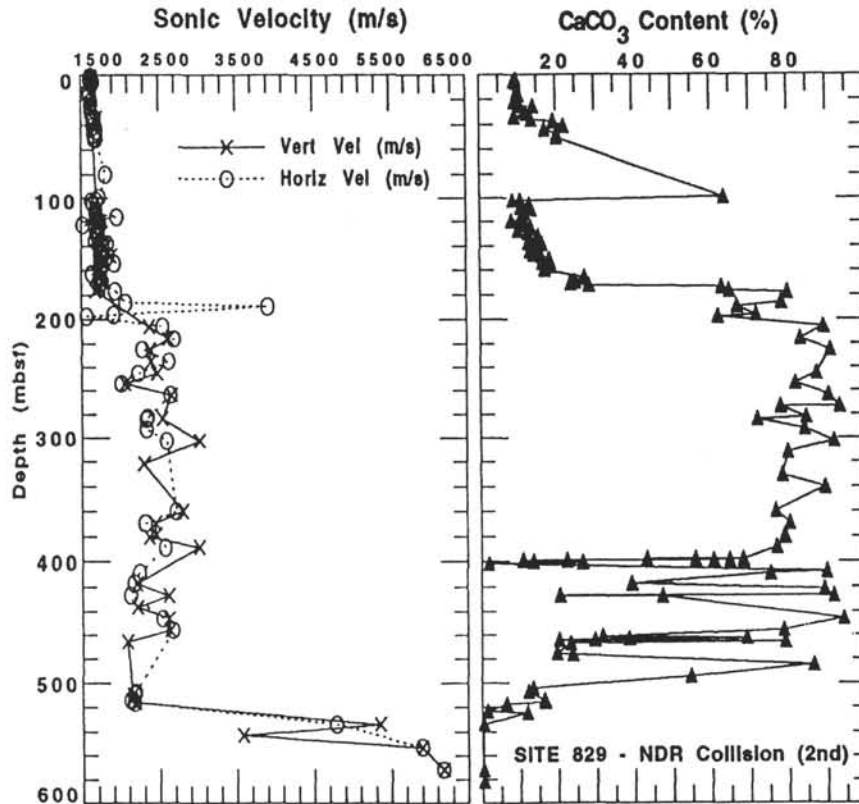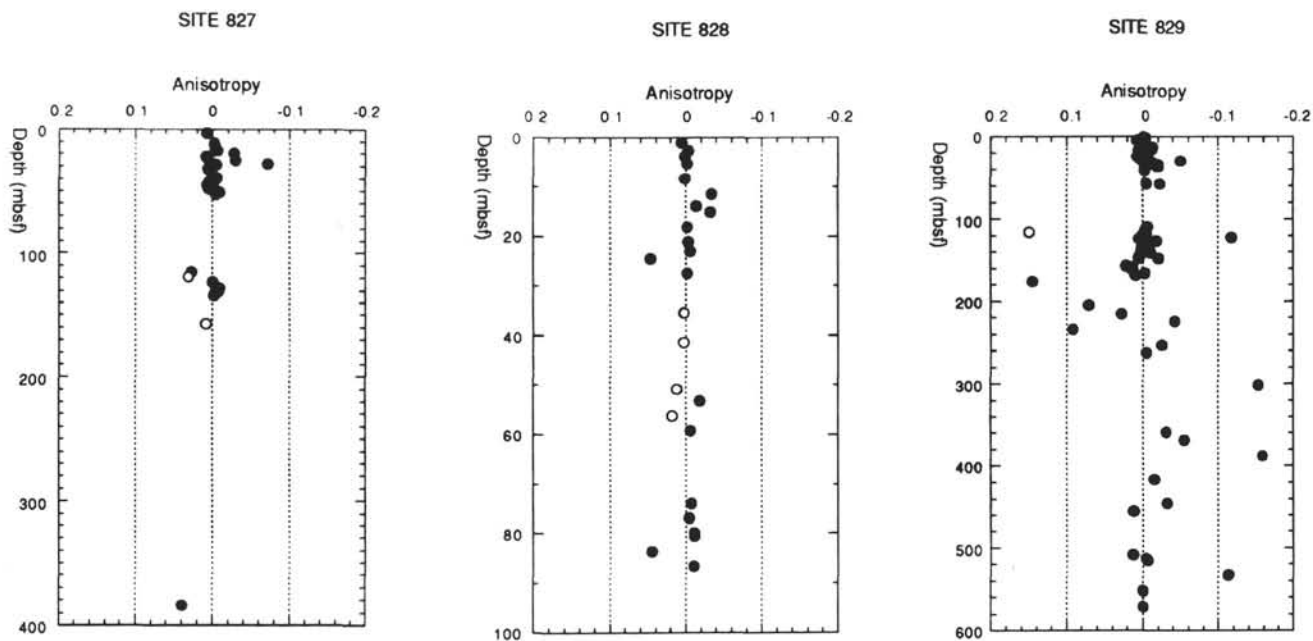

Figure 4 (continued).

SITE 827

SITE 828

SITE 829

Figure 5. Velocity anisotropy comparison of *A* values plotted vs. depth for NDR Sites 827, 828, and 829. Solid circles are compressional waves, open circles are shear waves. Note the increase in anisotropy at Site 829.

impinges on the central New Hebrides Island Arc (Fig. 1). Leg 134 drilled a 350.6 m thick succession through two lithostratigraphic units of Pleistocene to unknown age, gray-black to multi-colored volcanic silt, sand, sandstone, and breccia. Two tectonic units were defined that correlate with the lithostratigraphic units. We penetrated one shallow layer correlated with a seismic reflector that was previously thought to be a thrust fault, but due to hole collapse were not able to reach deeper east-dipping seismic reflectors that were thought to be accreted guyot fragments (Fisher, 1991). Lithostratigraphic interpretation at Site 830 suggests that Unit I (0–174.9 mbsf) consists of mostly unlithified sandy turbidites that were deposited along an unstable slope, and Unit II (174.9–350.6 mbsf) represents a highly geochemically altered epiclastic sequence whose components were derived from the nearby volcanic islands, Malakula and Espiritu Santo. These rocks, termed cataclasites, have undergone intense brittle deformation from tectonics and compression and show increasingly scaly fabric downhole (Shipboard Scientific Party, 1992). Metamorphic-like cataclasites are produced during the collision process by extreme fracturing, grinding, and shearing of rocks, conditions that have been documented in structural fabrics from other forearcs (Moore, 1986; Shreve and Cloos, 1986; Cloos, 1984). Cataclastic deformation often accounts for differences in biostratigraphic position and lithification of units.

Physical properties of the cores at Site 830 (Fig. 6) exhibit very definite downhole trends. Porosity and water content have high values of 72% and 85%, respectively, at the mudline, but decrease extremely rapidly in the first 50 mbsf to less than 40% porosity and 25% water content. Bulk density shows a corresponding sharp increase in the same interval (Unit IA, IB) from 1.60 Mg/m³ to 2.24 Mg/m³. Shear strength also increases rapidly within the upper 50 mbsf from 5 kPa to 135 kPa (Shipboard Scientific Party, 1992d). Below 50 mbsf, index properties continue along similar, but much more gradual trends with depth. In Unit II porosity steadies at about 25% and bulk density at 2.40 Mg/m³. Calcium carbonate content starts out at a low level at the seafloor and drops to almost zero through both units downhole.

Sonic velocities also increase rapidly in the first 50 mbsf from 1536 to 1688 m/s (Figure 6B), but the rate of increase then declines before reaching a maximum of 1962 m/s at the base of Unit I. Below 175 mbsf, velocities range widely, with high values near 4400 m/s. A change in the heterogeneity between the horizontal and vertical velocities also occurred at 175 mbsf. Unit I shows the same inverted

relationship between the vertical and horizontal compressional velocities (V_v and V_h; 8:5). Negative *A* values are slightly semi-isotropic (0.1–1.3%), while positive *A* values range from semi-isotropic to slightly anisotropic (0.1 to 0.52; Fig. 7). This reflects the lower porosities at Site 830, compared to the values of Sites 827 and 829 at comparable depths. In Unit II, anisotropy increases, with values for V_h significantly greater than V_v. The rapid decrease of porosity and water content and concomitant increase in bulk density, velocity, and shear strength strongly suggest that the collision of the Bougainville Guyot with the arc is inducing intense tectonic dewatering and lateral strengthening of the sediments at Site 830.

Site 831: Bougainville Guyot

Site 831 was drilled in the center of the Bougainville Guyot, a carbonate-capped, flat-topped seamount, which is the easternmost member of the SDC (Fig. 1). Site 831 is in 1066 m of water, 15 km due west of Site 830, 5 km west of the trace of the subduction zone, and 42 km southwest of the southern tip of Espiritu Santo Island. The guyot is forming a 10 km indentation in the slope where it impinges on the central New Hebrides forearc. Interpreted seismic reflection data indicate approximately 700 m of lagoon deposits as overlying the submerged basement volcano on which the coral reef had grown (Shipboard Scientific Party, 1992e). Site 831 was drilled to a total depth of 852 mbsf and can be separated into three lithostratigraphic zones: the soft pelagic sediment that covers the guyot cap (Unit I, 0–16.9 mbsf); the hard neritic corals that comprise lithostratigraphic Units II and III (16.9–727.5 mbsf); and the volcanic andesite breccia of Unit IV (727.5–852.0 mbsf), which forms the base of the guyot.

Physical properties data for Site 831 are plotted in Figure 8. Index properties vary widely from 0–20 mbsf, with water content ranging from 45%–90%, porosity 50%–75%, and bulk density 1.55–1.81 Mg/m³. Very little compaction appears to have occurred in the pelagic microfossils; minor lithology changes account for some of the wide range of index properties in Unit I. The basal contact of this unit (16–20 mbsf) is marked by an abrupt faunal transition from pelagic to hard, well-cemented neritic microfossils in Units II and III (16.9–727.5 mbsf), where core recovery dropped by 90%. The coral was probably fragmented and blown out by the rotating drill bit, so that only a few unoriented, cobble-sized neritic carbonate fragments (usually less than

1 m total) entered each core barrel. The guyot's distinct lithologic changes with depth are apparent in the velocity and $CaCO_3$ data (Fig. 8B). Soil horizons at 688.1 and 707.6 mbsf separate packstones from grainstones in Unit IIID, and the bottom of the carbonate sequence at 727.5 mbsf unconformably overlies weathered andesitic rocks in Unit IV. The contact with basement was also marked by an immediate increase in core recovery, from less than 10% to 30% or more, as well as an increase in the scatter of the physical properties data.

Because of the very low recovery in Units II and III (16.9–727.5 mbsf) index property measurements were very infrequent, about every 50–100 m. However, an excellent suite of downhole logs was obtained at this site, which helps to fill in gaps in the downhole picture (Shipboard Scientific Party, 1992e). When compared with the downhole logs (Fig. 9), we conclude that for the coral section (Units II and III) at Site 831, the discrete shipboard bulk density measurements are high relative to the RHOB-density log results. This may indicate that less dense material was fragmented and blown out of the hole ahead of the drill bit, while only the denser cobbles were competent enough to make it into the core barrel. Thus for the hard carbonates discussed below, the true in situ bulk density is lower (by about 0.4 Mg/m^3), and porosity and water content values probably higher, than indicated by these data from poorly recovered cores.

Overall water content in the hard coral from 16.9–727.5 mbsf is very low, ranging from 0% to 10.6%. Porosity decreased while bulk density and velocity increased in the hard coral with depth. Porosity ranges from 24.5% at 134 mbsf to 0% at 697.8 mbsf. Bulk density increases rapidly from 1.5 Mg/m^3 to 2.4 Mg/m^3 in the uppermost 80 m. Downhole measurements were made from about 80 to 800 mbsf, and the RHOB-density generally ranges from 2.1 Mg/m^3 to about 2.5 Mg/m^3 in the neritic carbonates (80–727 mbsf). Measured porosity increases somewhat in the subunits that have more visible molds and vugs. In the soil horizon at 688.1 mbsf, porosity and water content are relatively high (57.7% and 45%), and a sharp drop to about 1.60 Mg/m^3 is shown on the RHOB-density log.

The andesitic basement (Unit IV, 727.5–852.0 mbsf) is divided into five subunits in which physical properties vary widely according to the characteristics of the rock. Colorful cores in two subunits from 741–789 and 822–838 mbsf were dubbed "python rock" by the authors because they consist of black spots of andesitic hyalo-breccia surrounded by green palagonitic matrix. Porosity and water content values increased and bulk density and velocity decreased especially in the other three subunits from 727–741, 789–822, and 838–852 mbsf, which is less brightly colored andesite breccia that has been oxidized, reworked, and occasionally interbedded with grits and sandstones. The oxidized sections indicate periods in which the igneous base of the guyot was subaerially emergent prior to the buildup of the coral reef (Shipboard Scientific Party, 1992e; Baker et al., this volume), and physical properties correlate with this interpretation. Porosity and water contents are often higher and bulk density and velocities actually lower in weathered, oxidized sections than in the overlying carbonate units. Overall ranges in the basement rocks are 1.3%–20.2% for water content, porosity varies from 3.2%–36.1%, and bulk density ranges from 2.19–3.05 Mg/m^3. Velocity tracks with bulk density and is lower in the weathered subunits, varying widely between 3000 and 6000 m/s.

North Aoba Basin (NAB) Intra-arc Sites 832 and 833

Sites 832 and 833 were each drilled to depths of over 1000 mbsf into the center and the eastern flank, respectively, of the NAB (Fig. 1). Both sites are capped by volcanic sediment and ash of varying grain size. The difference in the sediment caps is their thickness, which is more than 350 m at Site 832 and only 85 m at Site 833. Similar differences in thickness of lithostratigraphic units from Site 832 to Site 833 are common and are related to the basin's symmetry (Shipboard Scientific Party, 1992f, g; Goud-Collins, this volume). The shallower units of the NAB are comprised of alternating succes-

sions of volcanic sediment, ash, and mixed sedimentary rocks interlayered with calcareous siltstone and chalks. A unit composed of basaltic breccia and volcanic sandstone occurs from 626–702 mbsf at Site 832 and from 375–578 mbsf at Site 833. The presence of basaltic sills from 832–1001 mbsf is unique to Site 833.

Site 832: Central NAB

Site 832 drilled two holes on the flat basin floor of the NAB in 3090 m of water, 45 km due south of the active Santa Maria volcano (which we observed emitting gray-white smoke), and about 50 km northeast of Espiritu Santo's Queiros Peninsula. Holes 832A and B were drilled to a total depth of 1106.7 mbsf and identified seven lithostratigraphic units from sediment and rocks which were mostly volcanic silts, sands, clays, and ash of Pleistocene to upper Miocene(?) age (Shipboard Scientific Party, 1992f). Physical property measurements at Site 832 (Fig. 10) were scattered, with only a very slightly decreasing porosity and water content gradient with depth from the mudline to below 300 mbsf (lithostratigraphic Units IA and IB). Porosity and water content in Unit I have high values of 40% and 80%, respectively. Bulk density ranges widely between 1.57 Mg/m^3 and 2.16 Mg/m^3. Sonic velocity varies as well, but shows little increase from 0–300 mbsf. Volcanic silty-ash layers in Unit I (0–206.2 mbsf in Hole 832A; 144.4–385.6 mbsf in Hole 832B) are the most porous, least consolidated, and contain the greatest amount of fluid of all material at Site 832. Vane shear strength values in this interval were also widely scattered, varying from 12.5 to 73.3 kPa (Shipboard Scientific Party, 1992f). A vane shear strength of 73.3 kPa would usually be typical of silty or carbonate sediment, but in any case is a very low value at 300 mbsf. The low vane shear values reflect numerous silty wet ash layers and the overall underconsolidated state of the sediment (Leonard, 1991) at Site 832, which is typical of an area of rapid sedimentation.

Below 320 mbsf, sediment becomes more lithified, with few unconsolidated ash layers. Overall index property scatter from 320 mbsf to the total depth of Site 832 (1106 mbsf) appears to result principally from small slumps and convoluted bedding, particularly from 350–600 mbsf (Units II and III), and due to normal faults with slickensides from 740–1040 mbsf (Units V, VI, and VII). These same units have $CaCO_3$ contents ranging from 0%–80% (Fig. 10B), due to numerous successions of foraminiferal and calcareous sedimentary rocks alternating with basaltic breccias and volcanic sandstones.

Immediately below 320 mbsf, values of bulk density and $CaCO_3$% increase sharply, and are associated with sedimentary pulses of lithified chalk, sandstone, and siltstone at the base of Unit IB. Sonic velocity also increases sharply in this subunit, reaching 3100 m/s. Below 320 mbsf, porosity and water content decrease very slowly downhole and maintain values that rarely fall below 40% and 25%, respectively, except from 385.6–461.5 mbsf (Unit II), and 625.7–702.0 mbsf (Unit IV). The most pronounced change in porosity and water content and concomitant increase in bulk density and sonic velocity at Site 832 occurs in Unit IV from 625–702 mbsf. This change is associated with a very hard, well-cemented sequence of basaltic breccias with volcanic siltstone and sandstone. A similar but less obvious trend occurs 200 m above in Unit II, which also consists of sandstone and breccia, suggesting that Unit II may be a less mature version of Unit IV. At 702 mbsf, a seismic unconformity of the basaltic breccias and sandstones in Unit IV with calcareous rocks below (Unit V) suggests that the former were volcanic products of the late Pliocene uplift of Espiritu Santo, emplaced as the DEZ began to collide with the New Hebrides arc (Shipboard Scientific Party, 1992f; Fisher et al., this volume).

In his examination of the relationship between physical properties and velocity anisotropy, Hamilton (1970) concluded that velocities in the horizontal plane (V_h) increase significantly at depths of 400 to 600 mbsf. At Site 832, compressional velocity anisotropy A values (Fig. 11) vary from 7.5% to –5.6% in Unit I (0–385.6 mbsf), but are generally semi-isotropic and positive. Such variations are most probably
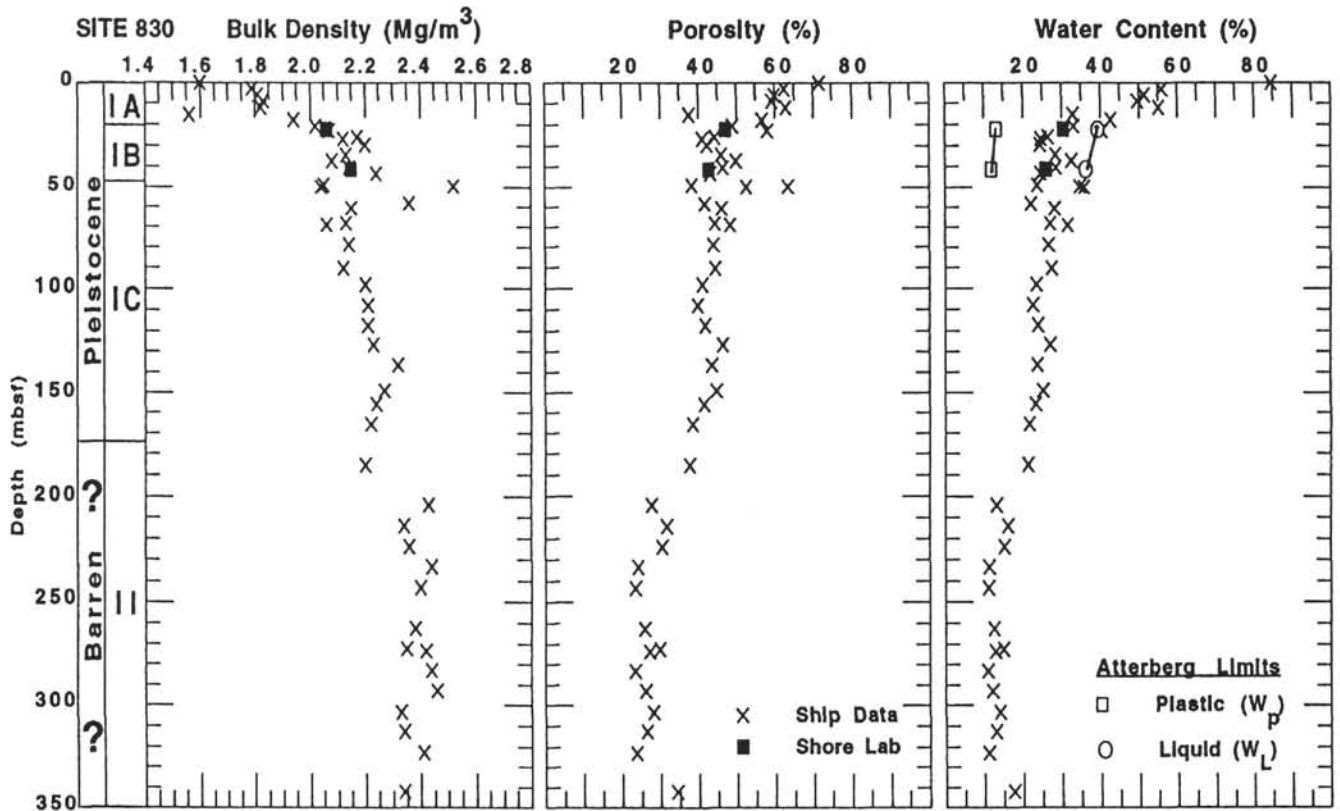
Figure 6. Physical properties plotted vs. depth for SDC collision Site 830, including age and lithostratigraphic units. Note very sharp decrease in porosity from 0–50 mbsf. Acoustic anisotropy at Site 830 was the largest among the seven Leg 134 sites.

related to lithology differences in the rapidly deposited volcanic silt and ash. The majority of the A values from 385–625.7 mbsf (Units II and III) are semi-isotropic, and the slightly positive A values correlate with the data of Hamilton (1970). Negative semi-isotropic A values were calculated mostly in the breccias from 625.7–702 mbsf (Unit IV), and correlate with similar values in breccias at Sites 829 and 831. A sharp positive anisotropy anomaly can be seen in Unit V from 700–860 mbsf. Using data from the downhole susceptibility tool, Roperch and Zhao (this volume), and Stokking et al. (this volume), measured magnetic susceptibility anisotropy, and calculated the ratio between the maximum magnetic axis and the average magnetic axis. These magnetic foliation measurements correlate well with the distinct increase in V_h, which causes the positive A values in Unit V. From 900–1100 mbsf, the deepest lithostratigraphic units (VI and VII) at Site 832, A-values are mainly semi-isotropic and vary between slightly positive and slightly negative.

Site 833: Eastern Flank of NAB

Site 833 was drilled in 2628 m of water on the flank of the NAB, 40 km east-southeast of Site 832 (Fig. 1). The site lies just 24 km northwest of the northern tip of rugged Maewo Island and about 72 km southeast of the smoking Santa Maria volcano. Site 833 was drilled with the intention of penetrating deeper, older basin strata of Miocene age, which are seen in outcrops on Maewo but could not be reached at Site 832 because of the thick cover of Pliocene and Quaternary sediments that fill the central NAB floor. Two holes were drilled through volcanic and calcareous mixed sedimentary rocks and basalt sills to a total depth of 1001.1 mbsf. Five lithostratigraphic units were identified in the cores before drilling terminated in lower Pliocene mixed sedimentary rock that had been intruded by basalt sills. Important keys to the divisions within the lithostratigraphic units are grain size of the volcanic sediment and ash, carbonate content, and

bioturbation (Shipboard Scientific Party, 1992g). Carbonate content and bioturbation are low when ash and sand content are high.

Physical properties measurements (Fig. 12) correlate with the lithostratigraphic units at Site 833 as well as at Site 832. However, sediment in the upper 375 mbsf (Units I and II) on the eastern flank of the NAB at Site 833 is slightly drier, less porous, and more dense than in the center of the basin at Site 832. Structural studies indicate that tectonic deformation and slumping has occurred on the basin flank from 0–375 mbsf (Shipboard Scientific Party, 1992f; Pelletier and Meschede, this volume; Goud Collins, this volume; Leonard, 1991). Physical properties results agree with this evidence. Porosity, water content, bulk density, and velocity are not as scattered and variable as at Site 832 and exhibit more normal trends with depth from 0–375 mbsf (Fig. 12). Porosity ranges mostly between 50% and 70%, water content 30% to 60%, and bulk density 1.70–2.10 Mg/m³. Sonic velocities remain below 2000 m/s down to 50 mbsf (Unit IIC), where a sharp increase matches an increase of bulk density and decreasing porosity and water content as the cores become more lithified calcareous claystone and siltstone (Fig. 12). At 376 mbsf a very sharp decrease in porosity to 20% and concurrent increase in bulk density to 2.50 Mg/m³ occurs and is associated with a downhole lithologic change from Pleistocene volcanic siltstone and calcareous claystone (Unit IID) to upper Pliocene coarse volcanic sandstone and basaltic breccia (Unit III). A sharp positive spike in velocity (5909 m/s) and decrease in CaCO₃% (Fig. 12B) also occurs at the top of Unit III at 400 mbsf. Bulk density and velocity remain high, while CaCO₃%, water content, and porosity are low throughout the sandstone/breccia section (Unit III and the top of Unit IV) to 600 mbsf. In Unit IV, a succession of calcareous mixed sedimentary rocks with numerous small faults, index properties are homogeneous, with porosity generally 40% and bulk density about 2.00 Mg/m³ from 600-830 mbsf. At 830 mbsf, the upper contact of the first basalt sill which intrudes Unit V, bulk density sharply increases to 2.60 Mg/m³ and velocity exceeds
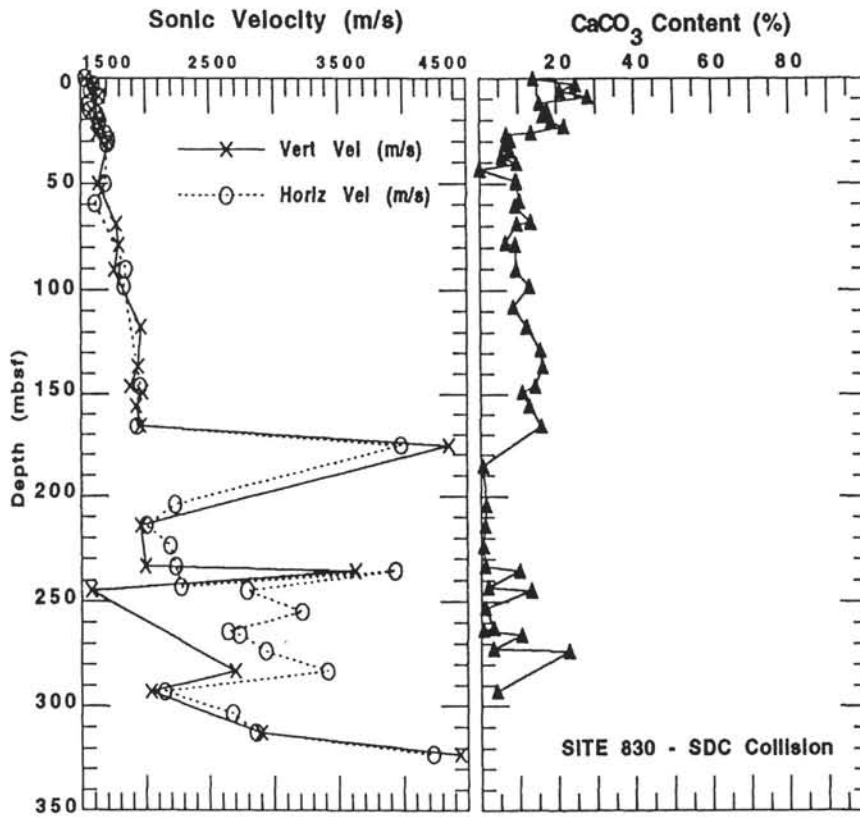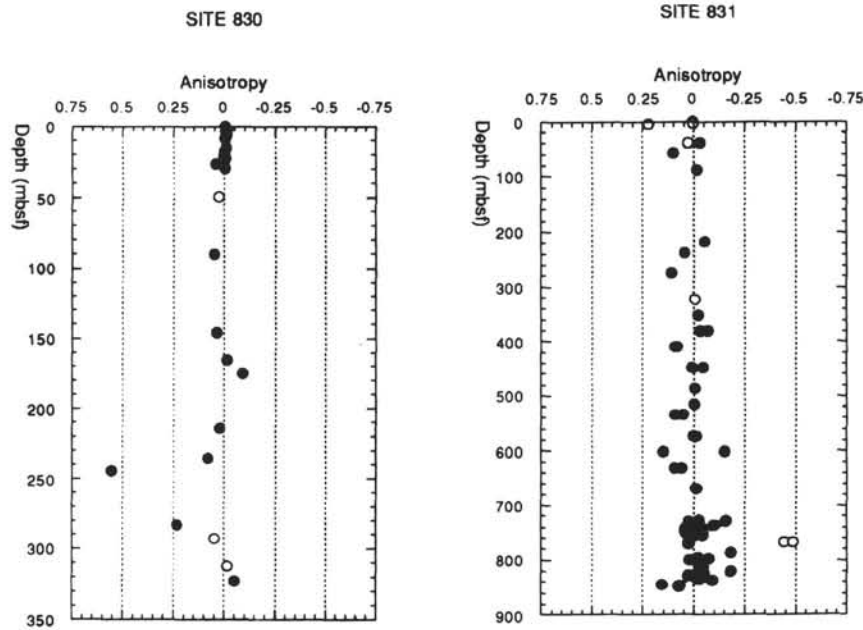
Figure 6 (continued).

Figure 7. Velocity anisotropy comparison of *A* values vs. depth for Sites 830 and 831. Solid circles are compressional waves, open circles are shear waves. Anisotropy increases significantly at Site 830 below 175 mbsf.

5500 m/s. Porosity and water content drop to less than 5% and remain low, except in short intervals where calcareous sedimentary rocks are not intruded by basalt sills. The interbedded calcareous sedimentary rocks and basalt sills account for the wide-ranging scatter in the physical properties data at the bottom (830–1001 mbsf) of Site 833.

Compared to the wide range of values at Site 832, Site 833 values for *A* (Fig. 11) are isotropic to slightly positive through 500 mbsf,

down to Unit III. Below this depth the base of Unit III shows negative *A* values in lithified volcanic sandstone comprised predominantly of coarse black basalt grains. Vertical and horizontal velocities show a more pronounced change from semi-isotropic to clear positive anisotropy in Unit IV from 600–830 mbsf, a unit with numerous small faults and interbeds of mixed sedimentary and volcanic rocks. In the lowermost 150 m (Unit V), *A* varies from positive to negative, with the nega-
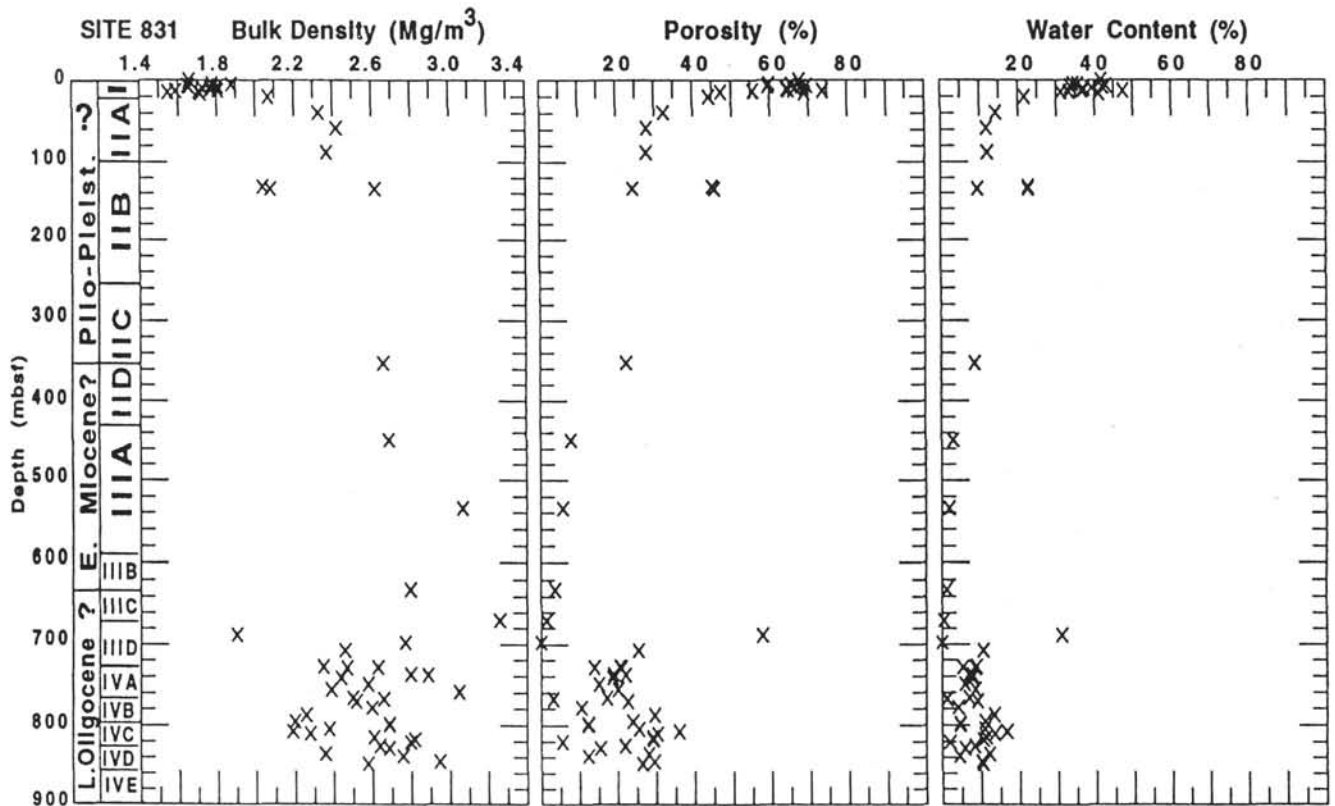
521

Figure 8. Physical properties plotted vs. depth for SDC Bougainville Guyot Site 831, including age and lithostratigraphic units. Some bulk density values are higher at the base of the carbonates than in the weathered andesite.

tive values found in the basalt sills, and positive, often anisotropic values in the calcareous sedimentary rocks that the sills intrude.

DISCUSSION

The Vanuatu sites drilled on Leg 134 are spread over different tectonic settings of an island arc system, and also over areas exhibiting different styles of tectonic deformation within the same setting. This is clearly reflected in the physical property results, particularly by the index properties. Sites drilled within the same setting show similar trends, chiefly Site 827 with Site 829, and Site 832 with Site 833. However, significant deviations are seen between the different sites, especially when there is a change of the tectonic domain or a change in the morphology within the same domain, such as Site 831 vs. Site 832, or Site 830 vs. Sites 827 and 829. The physical property values also change with lithology within the same domain, as for Sites 828 and 831. Similar lithologies often exhibit similar patterns of physical properties, even though magnitudes may differ. Fine-grained volcanic sediments at the sites have a fairly homogeneous trend of decreasing porosity with depth, with a similarly homogeneous trend of increasing bulk density (Site 827, 0–100 mbsf; Site 830, 50–150 mbsf). For measurements in chalk, limestone, foraminiferal and calcareous sedimentary rocks, porosity and bulk density values change little with depth (Site 829, 200–400 mbsf; Site 832, 462–626 mbsf). A third significant trend occurs in breccias, which produce a broad scatter in both porosity and bulk density data, reflecting measurements made in matrix and in the clasts (Site 829, 520–590 mbsf; Site 832, 620–700 mbsf).

Comparison of porosity values between the DEZ and NAB sites seems to suggest that the collision of the DEZ is responsible for the large decrease in porosity in the DEZ versus the NAB. Figure 13 uses smoothed data from six sites across the arc (except Bougainville Guyot, Site 831) to show the distinct decrease in porosity vs. total depth at the DEZ sites. The steepest and strongest decrease in porosity

is at Site 830, where the guyot is being subducted beneath the arc slope and compressing sediment in its path, followed by NDR Sites 829 and 827. In the upper units at Sites 827, 828, and 829 the silty volcanic sediments display a steady, near-vertical gradient of porosity. Site 828, the reference site on the NDR, shows evidence of higher porosity at depth in the foraminifer and nannofossil chalk units, which also have very high water content and appear to be channels for fluids coming out from the deformation front.

Figure 13 also shows how high porosity near the seafloor in the NAB decreases little with depth, especially in the center of the basin at Site 832. On the eastern flank of the NAB at Site 833, porosity remains high until a sharp drop occurs at about 350 mbsf, which is near the top of an interval of lithified, upper Pliocene volcanic sandstone breccia. Extensive diagenesis and hydrothermal alteration associated with elevated heat flow and higher thermal conductivity (Shipboard Scientific Party, 1992f) were measured at both NAB sites (Martin, this volume; Gerard, this volume). Lithification from diagenesis helps to explain the rapid decrease in porosity deep in the basin, below 600 mbsf at Site 832, and 400 mbsf at Site 833.

DEZ Collision Zone Sites 827–831

Index properties in volcanic sediments at Site 828 (Fig. 2) record a steady trend with no increase in bulk density or decrease in porosity from 0–58.7 mbsf (Unit I). Roperch and Zhao (this volume) discuss how magnetic susceptibility correlates with GRAPE density in the unlithified volcanic silts that comprise Unit I. Magnetic susceptibility is highest at the top of the section and decreases downhole, as do the volcanic components seen in the smear slide data (Shipboard Scientific Party, 1992a–e). These trends record the effects of plate convergence causing a lithology change in the silt. Volcanic components increase as the distance decreases between Site 828 and the New Hebrides Island arc. Thus, normal index properties trends of low bulk
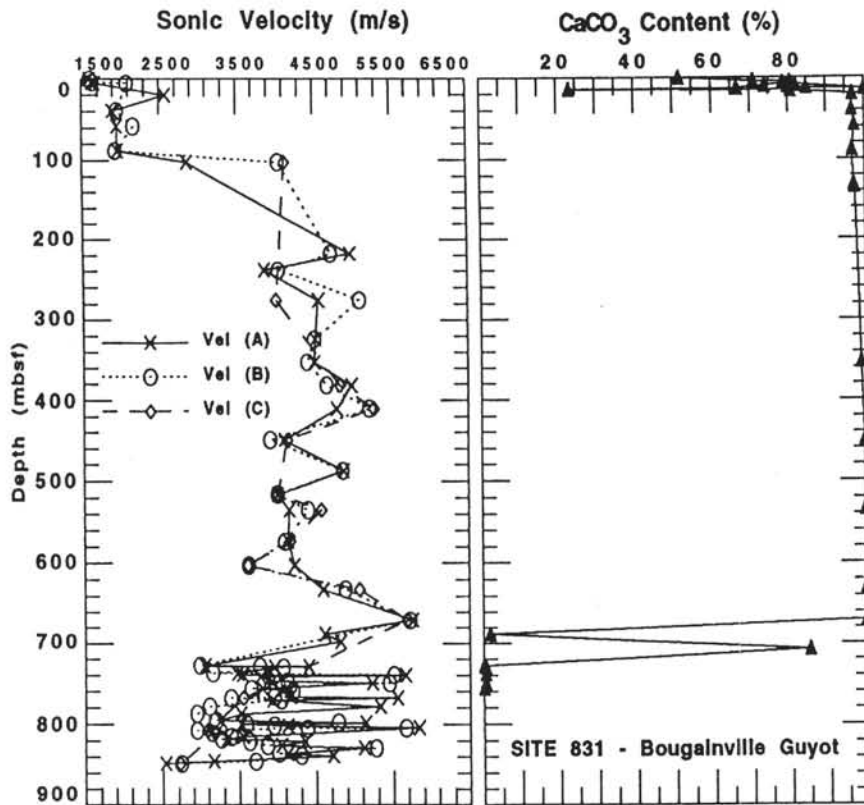
Figure 8 (continued).

density and high porosity are also cancelled by the increase of volcanic silt, in addition to missing overburden from slumping and compression of the sediment from tectonic effects. The increase of heavier minerals changes the normal compaction profile, and helps explain why the shallow bulk densities at the NDR sites are very high average values (Bryant et al., 1981) for sediments near the seafloor.

We estimate that recent slumping has removed 40-60 meters of overburden near the seafloor at Sites 828 and 829. Consolidation tests (Leonard, 1991) show that sediments at Sites 828 and 829 are very overconsolidated in the upper 60 mbsf, while the same type of volcanic sediments at Site 827 are normal to just slightly overconsolidated. Overconsolidation at the seafloor can result from physiochemical "origin cohesion" of surface material, but very overconsolidated sediment is more likely to indicate tectonic compression and/or overburden removal due to erosion or mass wasting. Sediment and fluid geochemistry results at Site 829 (Shipboard Scientific Party, 1992c; Martin, this volume) suggest that erosion of as much as 50 m of sediment must have occurred as a rapid and very recent slump. Geochemical gradients for alkalinity, calcium, and magnesium are similar at Sites 828 and 829, but not at Site 827. In the uppermost 50 mbsf at Site 830 (SDC collision), a rapid decrease in porosity occurs that is not seen from 0–50 mbsf at Sites 828 and 829. Thus, slumping must have eroded 40–60 m of the original surface interval at Sites 828 and 829, an area in which rapid vertical fluid flow due to tectonics facilitates mass wasting. Minor deposition and tectonic stress (Taylor, 1992) have occurred since the slump, and porosity gradients do not equilibrate as fast as the geochemical gradient. Older, deeper slumps at Site 827 (Fig. 3) caused by the oblique subduction of the NDR (Collot and Fisher, 1991), may account for the different consolidation profile in those sediments (Leonard, 1991).

Physical properties of sediment and rocks from Site 827 display an inverse correlation in the relationship between water content and porosity versus calcium carbonate content and thermal conductivity (Shipboard Scientific Party, 1992a). Water content and porosity are
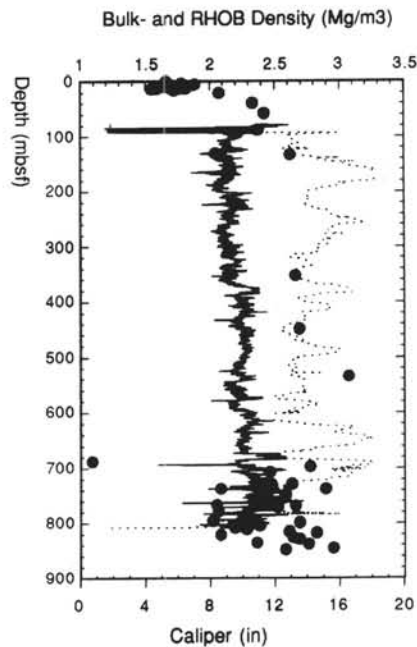

Figure 9. Bougainville Guyot Site 831 bulk-density values measured in situ by the RHOB-density downhole tool plotted vs. depth.

high in deformed zones from 107–252.6 mbsf (Units II and III) and in horizons where carbonate content is low (Fig. 3). In the tectonically deformed Unit III (141–252.6 mbsf), interpreted to consist entirely of accreted sediments (Reid et al., this volume), $CaCO_3$ content varies from 0%–45%. The largest shear zone at Site 827, from 230–252.6 mbsf, which is also an interval of generally low calcium carbonate con-
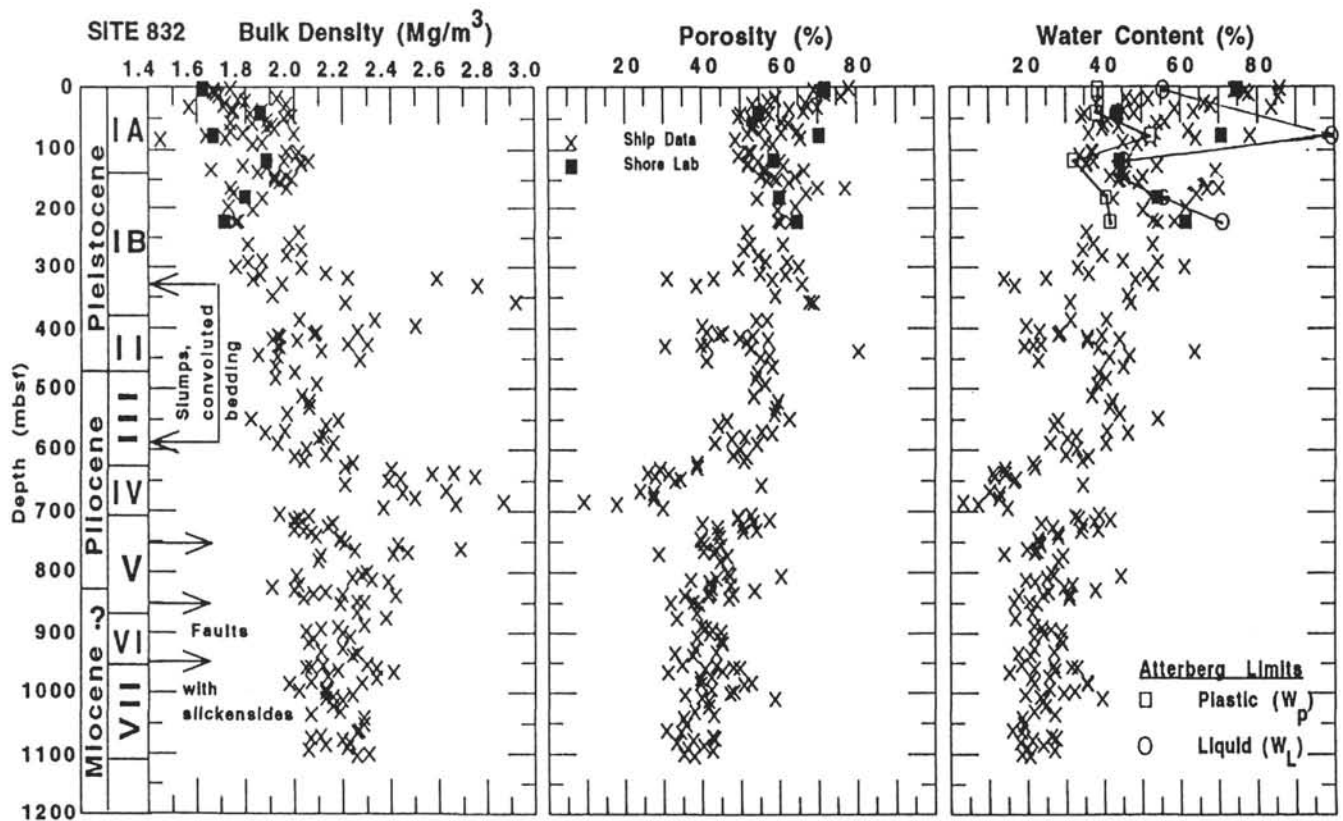
Figure 10. Physical properties vs. depth for central NAB Site 832, including age, lithostratigraphic units, and structural features (arrows).

tent, has several horizons of scaly cleavage fabric, especially around 243 mbsf (Meschede and Pelletier, this volume), where $CaCO_3$ is less than 10%. Below 252.6 mbsf (Unit IV), low porosity and water content and high bulk density and sonic velocity values reflect a marked change in lithology to an intensely deformed sed-lithic conglomerate with clasts of andesitic breccia. Overall at Site 827, tectonically induced shearing may occur preferentially in horizons of low $CaCO_3$%, and the shear zones may be serving as dewatering conduits for fluids.

From interpretation of multichannel seismic profiles of the area, Fisher (1986) suggested that the sedimentary section covering the NDR at Wousi Bank may represent a "collision complex," rather than an accretionary complex. He noted that the prism appears to exhibit seaward-dipping versus landward-dipping thrusts, and that more sediments may have been shed from the rapid uplift of Espiritu Santo and local volcanism than were being sheared from the NDR. In contrast to this interpretation, drilling at Site 829 showed that Vanuatu does represent an accretionary complex composed of at least eight imbricated thrust sheets consisting of alternating intervals of broken and shattered chalk with volcanic siltstone and highly sheared sedimentary breccia offscraped from the NDR. However, intervals of trench fill deposition due to collision are common (Reid et al., this volume). Structural studies (Meschede and Pelletier, this volume) indicate that deformation within the accretion-collision complex is concentrated along several major thrust zones marked by intervals of extreme tectonic deformation, several centimeters to several meters thick. Index property measurements in shear zones show sudden downhole increases in water content and porosity of as much as 20%, and the matrix in the thrust planes is nearly always a brown clay.

At reference Site 828, the lower Pliocene sediment on the NDR is a thin zone of unconsolidated foraminiferal ooze with a very high water content (>92%), but in the accretionary complex at Site 829, Pliocene sediment is a much thicker unit of foraminiferal chalk with very low water content (<20%). The difference in lithification and

thickness of these sediments may result from dewatering, heating, and thermally-induced consolidation of the ooze by extreme compressional stress, faulting, and channeling of fluids during tectonic accretion. Tectonically induced lateral compression is apparently taking place in the accretion/collision complex, resulting in pore volume reduction, sediment strengthening, and dewatering through fracture permeability. Lower matrix permeabilities and possible excess pore pressure in certain sedimentary units (Leonard, 1991) appear to channel fluid through more permeable, tectonically fractured lithologies. The low water content of the chalk below 200 mbsf at Site 829 is approximately half that of claystones and mudstones of similar depth at Site 671 in the Barbados complex (Mascle, Moore, et al., 1988; Leonard, 1989; Taylor and Leonard, 1990; Ask, 1991). This difference is due, in part, to sediments being incorporated into the complex from the DEZ that are more coarse-grained, less porous, and more permeable than the hemipelagic clay-dominated Barbados forearc. Because the décollement was not reached, we cannot use physical properties to directly address the question of why a detachment surface may develop at a particular stratigraphic horizon in this accretionary complex. However, the geochemical signature of pore water near the deepest thrust fault (522 mbsf) cored at Site 829 indicates that the fluid may have been derived from subduction related processes near the décollement (Martin, this volume).

The role of smectite in thrust fault development (Vrolijk, 1990) in the accretionary complex at Vanuatu is still unresolved. From mineral analyses of a few samples by Reid et al., (this volume) the brown clay is composed mainly of kaolinite, unlike Barbados (Tribble, 1990), where similar thrust fault zones contain mainly smectite. A more detailed clay mineral and sediment fabric analysis is needed, particularly for the shear zones and brown clay horizons at Site 829. There is also the question of which physical process came first: are the shear zones there because they developed in fluid-rich swelling clay horizons, or did the brown clay appear after the thrust occurred, as the
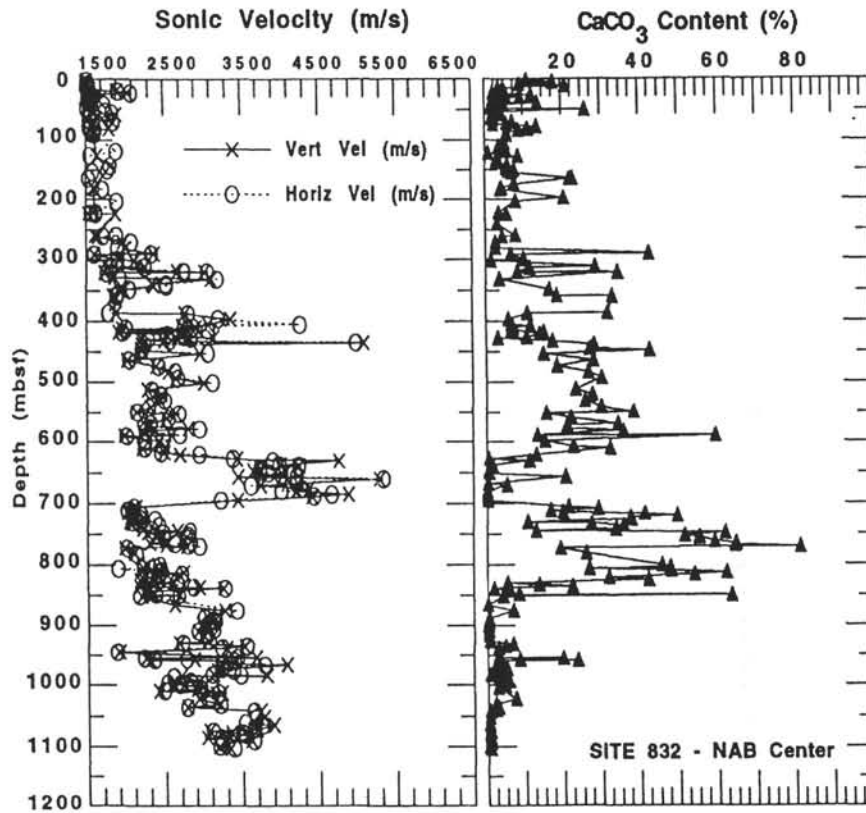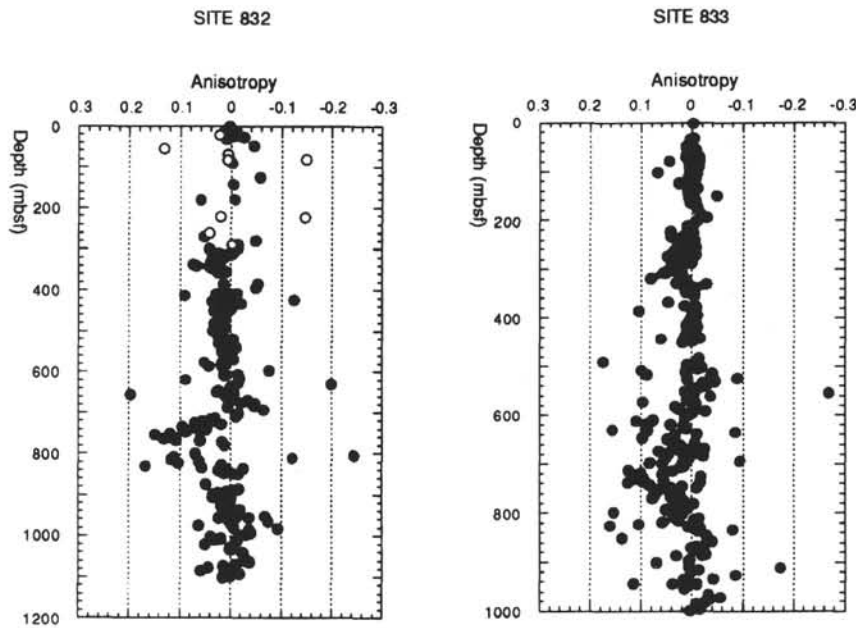
Figure 10 (continued).

Figure 11. Velocity anisotropy comparison of *A* values vs. depth for Sites 832 and 833. Solid circles are compressional waves, open circles are shear waves.

result of diagenesis within the fault plane? The décollement most probably is located where the sediment cover of the NDR meets the basement rocks, as the DEZ obliquely underthrusts the arc and sediment on the ridge is completely offscraped by collision with Espiritu Santo Island. Because Site 829 clays are similar in age and composition (Staerker, this volume; Reid et al., this volume) to brown

clay at the base of the pelagic sequence at Site 828, we suggest that these clays represent a preferred zone of separation, along which ridge sediment and rocks are detached from the downgoing plate and obducted onto the forearc slope.

Site 830, where the Bougainville Guyot impinges on the arc, represents a different style of deformation than the NDR. At Site 830,
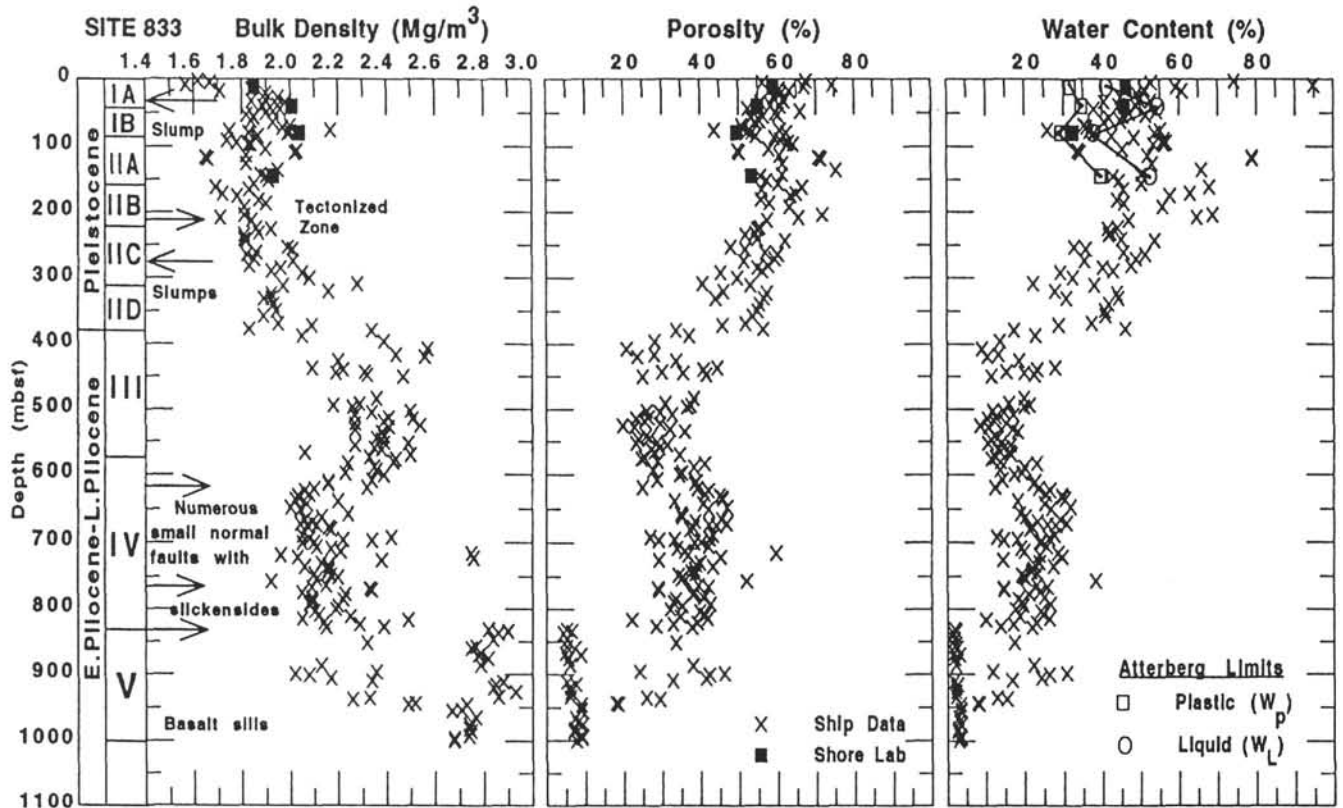
Figure 12. Physical properties vs. depth for eastern NAB flank Site 833, including age, lithostratigraphic units, and structural features (arrows).

tectonic compression is evident but no offscraping is apparent. A very strong decrease in water content and extreme geochemical fluid compositions with depth are further evidence that compressional dewatering from the impact of the guyot is taking place. Water content decreases from 84.7% at the seafloor to about 23% at 100 mbsf, and to 11% at 283.1 mbsf (Fig. 6A). Fracturing of volcanic rocks from collision facilitates increased diagenetic alteration and fluid flow. Foreshortening of the forearc resulting in the formation of imbricate thrust sheets allows sandy intervals and the thrust faults to act as conduits for mineral-rich fluids to escape (Shipboard Scientific Party, 1992d). Despite similar lithologies in apparently overconsolidated, volcanically-derived silt, water content at Site 830 is approximately half that at similar depths at Site 808 in the Nankai complex (Taira, Hill, Firth, et al., 1991; Taylor and Fisher, 1993).

Carlson and Christensen (1977) looked at Deep Sea Drilling Project (DSDP) data and suggested that the abrupt increase in anisotropy at depth implies that there is some correlation of anisotropy with compaction, and/or age and lithology of seafloor sediment. They concluded that the rapid increase in V_h with decreasing porosity implies that pore spaces affecting horizontal velocities are closed more rapidly by mineral reorientation, cementation, or recrystallization than are pore spaces affecting velocities in the vertical direction. Site 830 is the only site in the collision zone that shows the rapid decrease of porosity expected due to tectonic lateral stresses in accreting sediments (Fig. 6) and also the site where velocity anisotropy is most apparent (Fig. 7). The porosity data are similar to results presented by Bray and Karig (1985), who, after examining the Nankai Trough and other subduction zones, reported that low porosities in accretionary prisms are evidence that tectonic processes associated with accretion increase the efficiency of dewatering.

Coring at Site 830 had to be abandoned short of our 1000 mbsf objective due to drilling difficulties in material which, at 350 mbsf, was very lithified and highly geochemically altered. The sediment penetrated in Unit II (174.9–350.6 mbsf) is undated and unique for all the drilled sites, but is similar to rocks found on the island of

Malakula (Pelletier, pers. comm.). Although assumed to be derived from the nearby volcanic islands (Malakula and Espiritu Santo), exact origins are still poorly constrained. At the present collision rate of 13 cm/yr (Taylor et al., this volume), the start of subduction of the guyot is calculated to be upper Pleistocene, 0.15 Ma. Since then guyot slope has indented the arc slope by 10 km and formed a 5 km-wide anticline (Collot and Fisher, 1992). At Site 830, unlike the NDR, there is no evidence that any sediment we cored was accreted by the subduction of the SDC (Shipboard Scientific Party, 1992d). We speculate that if the sediment in this unit is derived from Malakula or other location in the central New Hebrides Island Arc, then the impingement of Bougainville Guyot probably would not have affected the sediment during initial deposition. If this is the case, then the fairly continuous gradients of index properties between 50 mbsf and the total sub-bottom depth (Fig. 6) may reflect the indentation of the guyot overprinting the signature of the original physical properties results.

The difference in the densities of the basement rocks accounts for the differences in the style of deformation at the locations where the twin ridges of the d'Entrecasteaux zone collide with the central New Hebrides Island Arc (Collot, Greene, Stokking, et al., 1992). The NDR consists of layered sedimentary rocks overlying a basement of Paleogene MORB (containing olivine, density >3.27 Mg/m^3). The Bougainville Guyot is an Eocene volcano composed of andesite breccia capped by over 700 m of coral reef and lagoonal sediment. Porosity and water content are low (<30%) except in the 20 m of lagoonal sediments on top of the guyot. Bulk densities in the igneous rock from 727.5–852 mbsf, which forms the base of the guyot, range from 2.19–3.05 Mg/m^3, depending on the amount of weathering and oxidation that the five different units of andesite breccia have undergone during periods of emergence. In addition, downhole RHOB-density results discussed earlier are consistently at least 0.4 Mg/m lower than these discrete values. Some carbonate density values, particularly near the base of the coral reef section, are actually higher than densities in the andesite breccia which comprises the volcanic base of the guyot (Figs. 8 and 9).
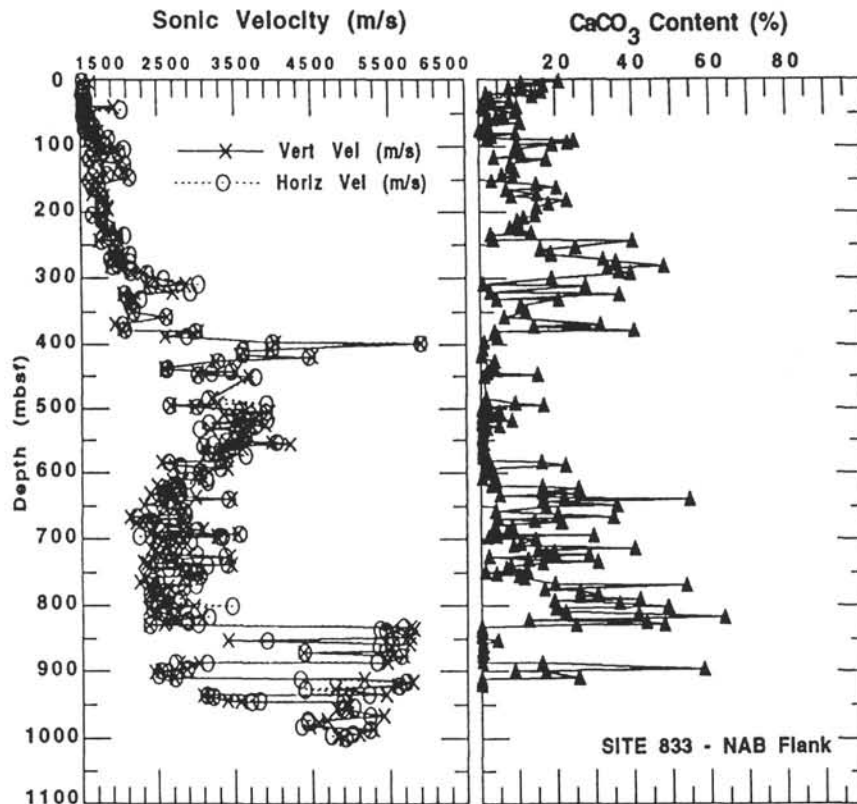
Figure 12 (continued).

Although discrete physical properties and downhole tool measurements just scratch the surface of the DEZ crust, they appear to confirm the observation (Collot, Greene, Stokking, et al., 1992) that the denser NDR is subducting and its sediment cover is being sheared off and accreted, while the more buoyant Bougainville Guyot is creating a large indentation in the arc slope and intensely overconsolidating (Leonard, 1991) sediments in its path.

Intra-arc Basin Sites 832–833

Rapid sedimentation occurred to deposit the upper 250 mbsf of material at Site 832 (Shipboard Scientific Party, 1992f). More than 350 m has been deposited in the last one million years, and this agrees well with the scattered high porosity and low bulk density values that were measured through this section. The upper 223 m of sediment at Site 832 is underconsolidated (Leonard, 1991), which is typical for sediment that is deposited very rapidly, because it does not have time to dewater. Velocity anisotropy, which varies from positive to negative (Fig. 11), may also result from the rapid sedimentation in this interval. Porosity varies with carbonate content; a small-scale increase in $CaCO_3\%$ is reflected in higher porosity values (Fig. 10), whereas an increase in the volcanic component in the sediment has an inverse effect on porosity. Deformational structures, found only below 300 mbsf, result from slumping, micro-faulting, and lateral compression processes within the NAB (Shipboard Scientific Party, 1992f; Pelletier and Meschede, this volume). Sharp increases in bulk density and concomitant decreases in porosity and water content occur in short intervals beginning at 318 (Unit IB), 386 (Unit II), and 625 mbsf (Unit IV) and are associated with lithologic units containing well cemented sandstone and basaltic breccia. The dense intervals bracket a generally more porous, less dense calcareous section with scattered index properties that mark convoluted bedding caused by tectonic events. These same events changed the inclination angle of the NAB's flanks, dislodging the sediments and forming slumps. Porosity decreases from 300–626

mbsf correlate with the numerous slump fold structures that occur in this interval, but micro-faulting is apparently not severe enough to affect pore volumes to the extent that it would be visible in the physical properties data. The porosity decreases may result from a combination of local compaction due to slumping, followed by lithification associated with the extensive diagenesis measured at both NAB sites (Martin, this volume). Elevated heat flow associated with higher thermal conductivity (Shipboard Scientific Party, 1992f, g) helps to explain the intense, caldron-like diagenetic alteration of the pore fluids in the deep basin at Sites 832 and 833.

The upper Pliocene basaltic breccia from 625–700 mbsf (Unit IV) may have been supplied by the initial eruption of the Central Chain volcanoes (Greene et al., this volume). A seismic stratigraphic unconformity at the top of Unit V at 702 mbsf appears to represent the time that uplift of Malakula and Espiritu Santo islands occurred in response to the collision of the DEZ with the New Hebrides Arc (Fisher et al., this volume). Below the 700 mbsf unconformity, the sedimentation rate drops from about 300 m/m.y., to less than 100 m/m.y. through 250 m of Pliocene to Miocene calcareous siltstone, limestone, and sandstone with steady, but scattered, index properties downsection. Unit III, above the unconformity from 461.5–625.7 mbsf, and Unit V, below it from 702–865.7 mbsf, have the highest calcareous components at Site 832 (Fig. 10B). Physical properties measurements support the interpretation that there was a change in the type of deposition and/or age below the unconformity at 702 mbsf. Unit V was probably deposited in quiet water, devoid of volcanic and terrestrially derived materials. Porosity and water content values are lower, and overall scatter in the index properties results from a large amount of small normal faults, which have propagated through these units due to the postdepositional depression of the basin caused by lateral compression from the collision of the DEZ (Pelletier and Meschede, this volume). Velocity measurements show a strong increase in horizontal velocity, which results in positive anisotropy. Roperch and Zhao (this volume) see a similar anomaly in the magnetic
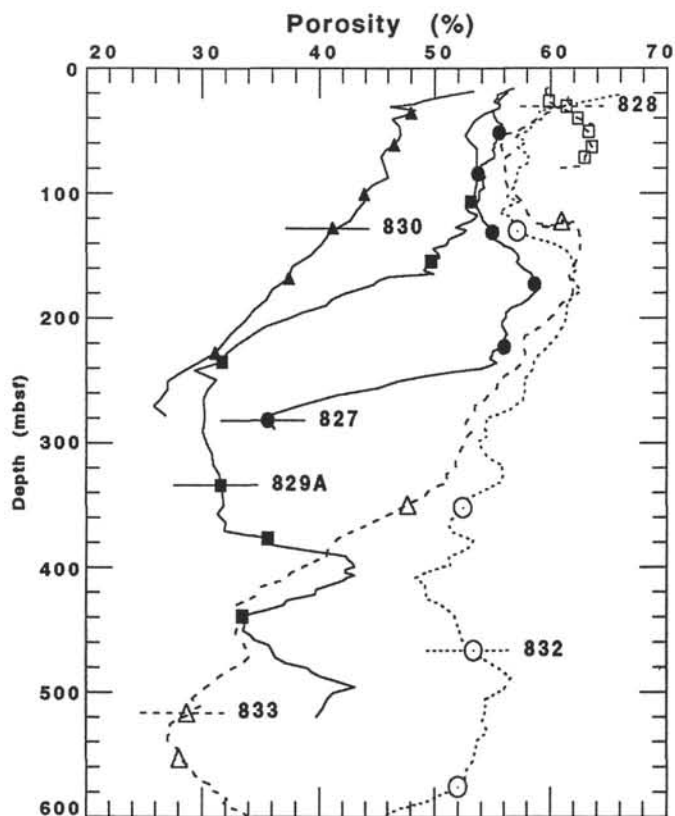
527

Figure 13. Summary of Leg 134 porosity data vs. depth for Sites 827–833, excluding Bougainville Guyot Site 831. Note the rapid porosity decrease at Sites 827, 829, and especially at 830, due to the collision of the DEZ.

foliation results from downhole susceptibility tool measurements. The foliation of grains results in high values of V_h relative to V_v. Because of lateral tectonic compression in addition to vertical overburden, the sonic pulse travels through increased grain contacts and decreased pore space ($V_{grain} > V_{water}$) than it would in material that is subject only to normal gravitational compaction. The combination of data sets (Fisher, 1986; Collot and Fisher, 1992; Collot, Greene, Stokking, et al., 1992) strongly support the suggestion that the breccia overlying the unconformity at 702 mbsf was emplaced as a result of the ridge-arc collision. Besides initially compacting the underlying calcareous sediment, heating and hydrothermal alteration since collision caused lithification and decreased porosity. Detailed analysis of the Nankai prism (Brückmann et al., 1993) reminds us that sources of acoustic anisotropy, particularly in tectonically active environments, are a complex combination of lithology, fabric, and microfaulting that are difficult to constrain. However, we believe that lateral compression of the basin from the DEZ collision is a major contributor to positive anisotropy at Site 832, which is stronger in the calcareous sediments immediately below the unconformity from 702–865.7 mbsf (Unit V) than it is in the volcanic sandstones from 865.7–952.6 mbsf (Unit VI). Much less CaCO₃% and more scatter in the physical properties from interbedded volcanic sandstone and breccia mark the section just above a 100 m interval of basaltic breccia encountered at the bottom of Site 832 (Unit VII). The basaltic breccia in Unit VII (952.6–1106.7 mbsf) appears to represent submarine volcanic eruptions associated with the initial formation of Espiritu Santo Island.

Lithostratigraphic units at Sites 832 and 833 generally correlate, but the similarities are not always obvious. Site 833 displays similar physical property trends with depth as at Site 832, but most differences can be attributed to basinal symmetry. Vane shear measurements (Shipboard Scientific Party, 1992g) were made to a depth of 261 mbsf in the center of the basin at Site 832, but were made only to 80 mbsf on the eastern flank of the basin because the cores became more lithified at shallower depths at Site 833. Sediment in the basin (Site 832) is underconsolidated, but sediment on the eastern flank of the NAB (Site 833) is overconsolidated to 40 mbsf and underconsolidated below that level (Leonard, 1991). The overconsolidated sediment most probably results from removal of a section of overburden by mass wasting, due to uplift of the flank of Maewo Island caused by compression across the basin.

Unresolved stratigraphic contradictions exist between Site 832 and Site 833 concerning the 702 mbsf unconformity seen in the seismic reflection profiles of the NAB (Shipboard Scientific Party, 1992f, g; Fisher et al., this volume). At Site 832, the seismic unconformity was interpreted to be located at 702 mbsf between Unit IV (breccia) and Unit V (limestone). At Site 833, physical properties (Fig. 12), together with lithostratigraphic and biostratigraphic results indicate that the equivalent horizon lies at 577.8 mbsf, the contact between Unit III (sandstone/breccia) and Unit IV (calcareous sediment/limestone). However, the seismic reflection data indicates that the unconformity between Units IV and V at Site 832 is acoustically equivalent to the 375.8 mbsf contact at Site 833 that separates Unit II (volcanic sediment) and Unit III (sandstone/breccia). In the volcaniclastic sediment in Unit II at Site 833, porosity and water content have a strong decreasing gradient, and bulk density and velocity a strong increasing gradient from 200–400 mbsf due to lithification of the cores. The next lower interval at Site 833 from 400–560 mbsf (Unit III) is a dense, dry, low porosity zone of upper Pliocene black volcanic sand and basaltic breccia, which suggest uplift and erosion of volcanic rocks from Maewo Island during that time. Interbedded volcanic and calcareous sandstones and mudstones from 578–830 mbsf, Unit IV at Site 833, have scatter in their index properties due to numerous small normal faults and variable lithologies, as at Site 832, Unit V. The apparent contradiction in the interpreted location of the unconformity may result from the fact that both Unit II, from 200–400 mbsf at Site 833, and Units III and IV, from 500–700 mbsf at Site 832, have strongly similar physical property gradients of decreasing porosity, along with increasing bulk density and sonic velocity. The strong resemblance in physical property trends in these intervals suggests that these similar trends are the reason that different units between the two sites correlate on seismic reflection profiles, even though this correlation is not supported by the stratigraphic data from the cores.

CONCLUSIONS

Although the décollement in the accretionary complex at Vanuatu was not penetrated by Leg 134 drilling, we speculate that the décollement most probably occurs where the sediment cover of the NDR meets the basement rocks, as the DEZ obliquely underthrusts the arc and the ridge is completely decapitated of its sediment by collision with Espiritu Santo Island and offscraped to form Wousi Bank. Because thin, soft layers of brown clay found in shear zones of the collision complex at Site 829 are similar in age and composition (Staerker, this volume; Reid et al., this volume) to brown clay at the base of the NDR pelagic sequence at Site 828, we suggest that these clays represent a preferred zone of separation, along which sediment and rocks from the ridge are detached from the downgoing plate and obducted onto the forearc slope.

Firm conclusions based on results from this study indicate the following for the Vanuatu region of the New Hebrides Island Arc:

1. Physical properties, together with evidence from stratigraphic, structural, and pore-fluid geochemistry data, indicate that tectonically induced lateral compression is taking place in the DEZ collision complex, resulting in pore volume reduction, sediment strengthening, and intense dewatering by fault-controlled fracture permeability.

2. Horizontal velocity anisotropy suggests that sediment and rocks in the DEZ and NAB are experiencing lateral compression as

a result of the arc-ridge collision. The general correlations in marine sediment between V_h and V_v at depth below the seafloor seen by Hamilton (1970) and Carlson and Christensen (1977) do not seem to be as strong for the Vanuatu sites as those authors reported, although the effects of lateral compression must certainly promote mineral reorientation, cementation, and recrystallization.

3. Porosity and water content values measured in the DEZ are low, indicating significantly less fluid exists in this accretionary complex than was found in other complexes such as the Barbados Ridge and Nankai Trough prisms. This difference is due in part to lithologic differences of the sediment being incorporated into the complex. Sediment in the DEZ is coarser grained, more porous, and more permeable than the pelagic clay-dominated Barbados forearc, or the generally fine-grained turbidites and mudstone of the Nankai prism. In the NAB, more fluids and higher porosity material bracketing indurated rocks suggest rapid burial and alteration of sediments during intense bursts of volcanism associated with tectonic subsidence of the basin due to lateral compression from collision.

4. Physical properties data supports other evidence suggesting that each ridge of the DEZ causes a different style of dewatering and forearc deformation. The denser NDR is subducting and its sediment cover is being offscraped and accreted, while the more buoyant Bougainville Guyot is indenting the arc and compressing sediments in its path.

5. Lithologic control on sediment physical properties seems to be a principal factor influencing accretion, subduction, and the location of the décollement zone in accretionary prisms. Fluid content in DEZ sediment at equivalent depths is about half that of sediment in the Barbados and Nankai complexes. Despite lithologic variations between the prisms, the low water content suggests that increased dewatering at certain locations along convergent margins is due to compressional stresses from collision with a ridge or a seamount which are greater than the stresses created by normal subduction of ocean floor.

ACKNOWLEDGMENTS

REFERENCES*

Andrews, J.E., Packham, G., et al., 1975. *Init. Repts. DSDP,* 30: Washington (U.S. Govt. Printing Office).

Ask, M.V.S., 1991. Water content and porosity of sediments and rocks in the New Hebrides and Lesser Antilles convergent margins [M.S. thesis]. Luleå Univ. of Technology, Luleå, Sweden.

ASTM, 1989. *Annual Book of ASTM Standards for Soil and Rock; Building Stones: Geotextiles* (Vol. 04.08): Philadelphia (Am. Soc. Testing Materials), 168–862.

Boyce, R.E., 1976. Definitions and laboratory techniques of compressional sound velocity parameters and wet-water content, wet-bulk density, and porosity parameters by gravimetric and gamma ray attenuation techniques. *In* Schlanger, S.O., Jackson, E.D., et al., *Init. Repts. DSDP,* 33: Washington (U.S. Govt. Printing Office), 931–958.

Bray, C.J., and Karig, D.E., 1985. Porosity of sediments in accretionary prisms, and some implications for dewatering processes. *J. Geophys. Res.,* 90:768–778.

Brückmann, W., Moran, K., and Taylor, E., 1993. Acoustic anistropy and microfabric development in accreted sediment from the Nankai Trough. *In* Hill, I.A., Taira, A., Firth, J.V., et al., *Proc. ODP, Sci. Results,* 131: College Station, TX (Ocean Drilling Program), 221–233.

Bryant, W.R., Bennett, R.H., and Katherman, C.E., 1981. Shear strength, consolidation, porosity, and permeability of oceanic sediments. *In* Emiliani, C. (Ed.), *The Sea* (Vol. 7): *The Oceanic Lithosphere:* New York (Wiley), 1555–1616.

Carlson, R.L., and Christensen, N.I., 1977. Velocity anisotropy and physical properties of deep-sea sediments from the western South Atlantic. *In* Supko, P.R., Perch-Nielsen, K., et al., *Init. Repts. DSDP,* 39: Washington (U.S. Govt. Printing Office), 555–559.

Cloos, M., 1984. Landward-dipping reflectors in accretionary wedges: active dewatering conduits? *Geology,* 12:519–522.

Collot, J.-Y., and Fisher, M.A., 1991. The collision zone between the North d'Entrecasteaux Ridge and the New Hebrides Island Arc. Part 1: Seabeam morphology and shallow structure. *J. Geophys. Res.,* 96:4457–4478.

————, 1992. The d'Entrecasteaux Zone-New Hebrides Island Arc collision zone: an overview. *In* Collot, J.-Y., Greene, H.G., Stokking, L.B., et al., *Proc. ODP, Init. Repts.,* 134: College Station, TX (Ocean Drilling Program), 19–31.

Collot, J.-Y., Greene, H.G., Stokking, L.B., et al., 1992. *Proc. ODP, Init. Repts.,* 134: College Station, TX (Ocean Drilling Program).

Fisher, M.A., 1986. Tectonic processes at the collision of the d'Entrecasteaux zone and the New Hebrides island arc. *J. Geophys. Res.,* 91:10470–10486.

————, 1991. Structure of the collision zone between the Bougainville Guyot and the accretionary wedge of the New Hebrides Island Arc, Southwest Pacific. *Tectonics,* 10:887–903.

Greene, H.G., Collot, J.-Y., Pelletier, B., and Lallemand, S., 1992. Observation of forearc seafloor deformation along the north d'Entrecasteaux Ridge-New Hebrides Island Arc collision zone from *Nautile* submersible. *In* Collot, J.-Y., Greene, H.G., Stokking, L.B., et al., *Proc. ODP, Init. Repts.,* 134: College Station, TX (Ocean Drilling Program), 43–53.

Greene, H.G., Macfarlane, A., Johnson, D.A., and Crawford, A.J., 1988. Structure and tectonics of the central New Hebrides Arc. *In* Greene, H.G., and Wong, F.L. (Eds.), *Geology and Offshore Resources of Pacific Island Arcs—Vanuatu Region.* Circum-Pac. Counc. Energy Miner. Resour., Earth Sci. Ser., 8:377–412.

Hamilton, E.L., 1970. Sound velocity and related properties of marine sediments, North Pacific. *J. Geophys. Res.,* 75:4423–4446.

Katz, H.R., 1988. Offshore geology of Vanuatu-previous work. *In* Greene, H.G., and Wong, F.L. (Eds.), *Geology and Offshore Resources of Pacific Island Arcs—Vanuatu Region.* Circum-Pac. Counc. Energy Miner. Resour., Earth Sci. Ser., 8:93–124.

Leg 134 Shipboard Scientific Party, 1991. Material transfer in an arc-ridge collision zone. *Eos,* 72:425.

Leonard, J.N., 1989. Consolidation, permeability, and geotechnical properties of Ocean Drilling Program Leg 110 sediments from the Barbados forearc. [M.S. thesis]. Texas A&M Univ., College Station, TX.

————, 1991. Physical and geochemical properties of seafloor sediments from the Vanuatu collision zone in the central New Hebrides Island arc, South Pacific Ocean [Ph.D. dissert.]. Texas A&M Univ., College Station, TX.

Luyendyk, B.P., Bryan, W.B., and Jezek, P.A., 1974. Shallow structure of the New Hebrides island arc. *Geol. Soc. Am. Bull.,* 85:1287–1300.

Mascle, A., Moore, J.C., et al., 1988. *Proc. ODP, Init. Repts.,* 110: College Station, TX (Ocean Drilling Program).

Moore, J.C. (Ed.), 1986. *Structural Fabric in Deep Sea Drilling Project Cores From Forearcs.* Mem.—Geol. Soc. Am., 166.

ODP Leg 131 Scientific Drilling Party, 1990. Accretion: ODP at the leading edge. *Geotimes,* 35:18–24.

ODP Leg 134 Scientific Drilling Party, 1991. Documenting twin-ridge collision and arc deformation. *Geotimes,* 36:23–25.

Shipboard Scientific Party, 1992a. Site 827. *In* Collot, J.-Y., Greene, H.G., Stokking, L.B., et al., *Proc. ODP, Init. Repts.,* 134: College Station, TX (Ocean Drilling Program), 95–137.

————, 1992b. Site 828. *In* Collot, J.-Y., Greene, H.G., Stokking, L.B., et al., *Proc. ODP, Init. Repts.,* 134: College Station, TX (Ocean Drilling Program), 139–177.

————, 1992c. Site 829. *In* Collot, J.-Y., Greene, H.G., Stokking, L.B., et al., *Proc. ODP, Init. Repts.,* 134: College Station, TX (Ocean Drilling Program), 179–260.

---

*Abbreviations for names of organizations and publications in ODP reference lists follow the style given in *Chemical Abstracts Service Source Index* (published by American Chemical Society).

————, 1992d. Site 830. *In* Collot, J.-Y., Greene, H.G., Stokking, L.B., et al., *Proc. ODP, Init. Repts.,* 134: College Station, TX (Ocean Drilling Program), 261–315.

————, 1992e. Site 831. *In* Collot, J.-Y., Greene, H.G., Stokking, L.B., et al., *Proc. ODP, Init. Repts.,* 134: College Station, TX (Ocean Drilling Program), 317–386.

————, 1992f. Site 832. *In* Collot, J.-Y., Greene, H.G., Stokking, L.B., et al., *Proc. ODP, Init. Repts.,* 134: College Station, TX (Ocean Drilling Program), 387–477.

————, 1992g. Site 833. *In* Collot, J.-Y., Greene, H.G., Stokking, L.B., et al., *Proc. ODP, Init. Repts.,* 134: College Station, TX (Ocean Drilling Program), 479–557.

Shreve, R.L., and Cloos, M., 1986. Dynamics of sediment subduction, melange formation, and prism accretion. *J. Geophys. Res.,* 91:229–245.

Taira, A., Hill, I., Firth, J.V., et al., 1991. *Proc. ODP, Init. Repts.,* 131: College Station, TX (Ocean Drilling Program).

Taylor, E., and Fisher, A., 1993. Sediment permeability at the Nankai Accretionary Prism, Site 808. *In* Hill, I.A., Taira, A., Firth, J.V., et al., *Proc. ODP, Sci. Results,* 131: College Station, TX (Ocean Drilling Program), 235–245.

Taylor, E., and Leonard, J., 1990. Sediment consolidation and permeability at the Barbados forearc. *In* Moore, J.C., Mascle, A., et al., *Proc. ODP, Sci. Results,* 110: College Station, TX (Ocean Drilling Program), 289–308.

Taylor, F.W., 1992. Quaternary vertical tectonics of the central New Hebrides Island Arc. *In* Collot, J.-Y., Greene, H.G., Stokking, L.B., et al., *Proc. ODP, Init. Repts.,* 134: College Station, TX (Ocean Drilling Program), 33–42.

Tribble, J.S., 1990. Clay diagenesis in the Barbados Accretionary Complex: potential impact on hydrology and subduction dynamics. *In* Moore, J.C., Mascle, A., et al., *Proc. ODP, Sci. Results,* 110: College Station, TX (Ocean Drilling Program), 97–110.

Vrolijk, P., 1990. On the mechanical role of smectite in subduction zones. *Geology,* 18:703–707.